Whole-body Kinematics: Response Comparison of the Hybrid III and Hybrid III Pedestrian ATD in DRoTS Rollover Tests

Qi Zhang, Jason Kerrigan, David Lessley, Jeremy Seppi, Patrick Riley, Patrick Foltz, Jack Lockerby, Brian Overby, Christopher Sowers, Jeff Crandall

Abstract The goal of this study was to quantify and examine differences between the whole-body occupant kinematics of the Hybrid III 50th Percentile Male ATD and the Hybrid III 50th Percentile Pedestrian ATD in controlled laboratory tests aimed at simulating the airborne phase of a rollover crash. Eight pure roll tests (without ground impact) were performed where a vehicle test buck, which was pitched front-end down by 5 degrees, was rotated at a quasi-static, low (180 deg/s) or high (360 deg/s) roll rate (pure rotation tests). In each test, one of the two ATDs was seated in either the trailing- or leading-side front-row seat with three-point belt restraints. ATD kinematics was measured using a 500-Hz 26-camera 3D motion capture system. The buck and ATD kinematics were highly repeatable in these tests. Both ATDs, generally, drifted outboard and upward as a result of the rotations applied, and the ATD torso also pitched forward, which moved the head forward and the pelvis rearward. The ATD kinematics and excursion were the combined result of centrifugal acceleration (from the buck's rotational motion), gravity and inertia (acceleration and deceleration of the buck). It was also observed that the Hybrid III Pedestrian ATD had a smaller vertical excursion and forward pitch rotation, but larger lateral excursion compared to the Hybrid III ATD. This study established a repeatable methodology for measuring occupant kinematic response when vehicle kinematics simulated rollover crashes, which can be used to facilitate rollover occupant kinematics analysis, ATD biofidelity assessment and computational model validation.

Keywords biofidelity, DRoTS, Hybrid III, kinematics, pedestrian, rollover

I. INTRODUCTION

Though rollover occurs in only 2.2% of all motor vehicle crashes, these crashes are responsible for over one third of all motor vehicle crash fatalities [1]. Numerous previous research studies have utilized anthropometric test devices (ATD) to study occupant dynamics and injury risk in rollover crashes [2-5]. While the 50th percentile male Hybrid III ATD was designed to predict occupant kinematics and injury risk in frontal crashes, it has been frequently used for rollover crash research. In addition, the Hybrid III ATD has been modified to incorporate the Hybrid III Pedestrian pelvis in some studies since increased hip mobility was anticipated to offer more realistic ATD kinematics than the standard pelvis [6]. However, very few studies have been performed to evaluate differences between ATD responses or to establish baseline biofidelity of the ATDs in rollover crashes. Moffatt et al. [6-7] conducted tests with the Hybrid III ATD, the Hybrid III ATD with a pedestrian pelvis, human volunteers and a cadaver to measure and compare head excursions between the subjects in pure rotation tests. The authors compared vertical head excursions between the subjects as a means of evaluating ATD biofidelity and restraint system characteristics. While the magnitude of head vertical excursion can influence injury risk, a biofidelity analysis that examines whole-body three-dimensional motion provides for a more complete basis on which to evaluate subject variations. Consideration of multiple body segment kinematics ensures that intersegment stiffness is assessed, and three-dimensional analysis permits examination of not only vertical but also lateral and out-of-plane motion, which can affect occupant position and orientation at impact, and thus injury risk.

Q. Zhang is Graduate Research Assistant (tel:1-434-296-7288x152; fax:1-434-296-3453; qz5za@virginia.edu), J. Kerrigan is Senior Scientist, D. Lessley and P. Riley are Research Scientists, J. Seppi and J. Lockerby are Graduate Research Assistants, P. Foltz, B. Overby and C. Sowers are Research Assistants, all at the University of Virginia Center for Applied Biomechanics. Prof. J. Crandall is the Director of the Center.

The current study is the first part of a multi-step research effort aimed at evaluation of whole-body kinematic and kinetic biofidelity of existing ATDs in rollover crashes. This initial step compares only the Hybrid III and the Hybrid III Pedestrian ATDs in non-impact, roll-only, tests, whereas future efforts will consider other ATDs, cadavers, and impact and simulated impact rollover tests. Tests were conducted using a vehicle test buck developed to mimic the inertial, geometric and strength properties of a full-sized crossover developed for the US market [8-9]. Roll motions of the buck were powered using the Dynamic Rollover Test System (DRoTS) [10]. The goals of this study were: 1) to evaluate the repeatability of the vehicle buck roll-only test methodology and 2) to quantify and examine differences between the whole-body occupant kinematics of the 50th percentile Male Hybrid III ATD and the 50th percentile Male Hybrid III Pedestrian ATD.

II. METHODS

Test System

The tests were conducted using the DRoTS test fixture, which was constructed to perform controlled, repeatable, rollover crash tests with full vehicles inside a laboratory [10]. A parametric rollover test buck was developed for use with DRoTS to investigate ATD biofidelity in rollover crash tests (Appendix, Figure 1A). It was designed to have a rigid base, consisting of all the components below the simulated vehicle belt line, and a deformable (and thus replaceable) roof structure, consisting of all the components above the belt line (roof, pillars, headers and cross beams). The base structure (Appendix, Figure 1A) consisted of A-, B-, C- and D-pillars, front and rear pillar connections, and removable “doors.” The pillars and roof of the buck were not used in this study, since no vehicle-to-ground impact occurred in the tests, and the absence of the roof facilitated use of an optical 3D motion capture system that relied upon line-of-sight from off-board cameras to onboard targets.

The buck was designed to mimic the inertial properties and exterior and interior geometry of 15 late-model full-sized crossover or mid-sized sport utility vehicles (SUV) from the United States fleet. Interior geometry of the fleet vehicles, which were determined from consumer marketing materials, was determined to vary only minimally across the entire set of 15 vehicles (maximum coefficient of variation for any measurement was 6%). As a result, detailed measurements were made manually on one of the 15 vehicles to determine specific interior geometric dimensions for the buck including seat position relative to the roof, pillars, console and instrument panel, and overall interior width/height/length and door opening geometry. Simple rigid seats, knee bolsters, toe pans, belt D-ring mounting posts and a center console were designed to generally match the interior geometry of the vehicles. The flat sheet aluminum seat pan was divided between front and rear sections to facilitate boundary condition instrumentation. The seatback, which was fixed with a 15 degree rearward pitch, was constructed of two pieces of steel tubing with four adjustable clamps (two on each tube) that held rounded aluminum blocks cantilevered interiorly and protruding toward the ATD’s back (Appendix, Figure 2A). The seat configuration was used to improve visualization of the posterior aspect of each ATD and minimize any hindrances to ATD motion. A three-point fixed-length restraint (without retractor) was used in each ATD seating position. The locations of the outboard lap belt anchors and the shoulder belt D-rings relative to the seats were specified to match the geometry of one of the vehicles used in designing the buck. The inboard shoulder/lap belt anchor was oriented symmetric to the outboard anchor (Appendix, Figure 2A Left). The D-ring, buckle and latch plate were standard vehicle parts from a MY 2012 truck (Takata, Inc.) and the belt webbing has been used and characterized previously [11] (Narricot Industries, International twill pattern 13195, 6-8% elongation, 26.7 kN minimum tensile strength). The belt webbing was anchored to the vehicle at the outboard lap belt attachment and at the base of the B-pillar with turnbuckles that facilitated pretest tensioning of both ends.

Instrumentation

Buck instrumentation: The buck was outfitted with an inertial measurement unit containing three accelerometers (Endevco 7290E-30, Meggitt Sensing Systems, San Juan Capistrano, CA) measuring accelerations about the sensor unit’s local X, Y and Z component directions. Additionally one 1500 deg/s (sensor X axis) and two 300 deg/s (sensor Y and Z axes) angular rate sensors were included to measure angular velocities about the same local sensor cube axes (DTS ARS-1500 or ARS-300, Diversified Technical Systems, Seal Beach, CA). The sensor unit's local axes were aligned with the buck's local coordinate axes. A roll encoder was also installed in the rotational axis of the buck to measure buck rotation angle.

Hybrid III 50th and Hybrid III 50th Pedestrian: The Hybrid III 50th dummy (H3) and the Hybrid III 50th Pedestrian dummy (H3P) were used in this study (Figure 1). The H3P ATD is a modification of the original H3 ATD for the purpose of vehicle-pedestrian impact testing. The H3P is similar to the H3, except the H3P has a straight instead of curved lumbar spine, with one instead of two steel cables, the H3P pelvis flesh is not molded in the seating position like the H3, it has articulating hip segments that are detached from the pelvis, and the H3P has a different knee joint (Figure 1). For each test, one ATD was seated in one front row seating position and the other ATD was seated in the other front row seating position.

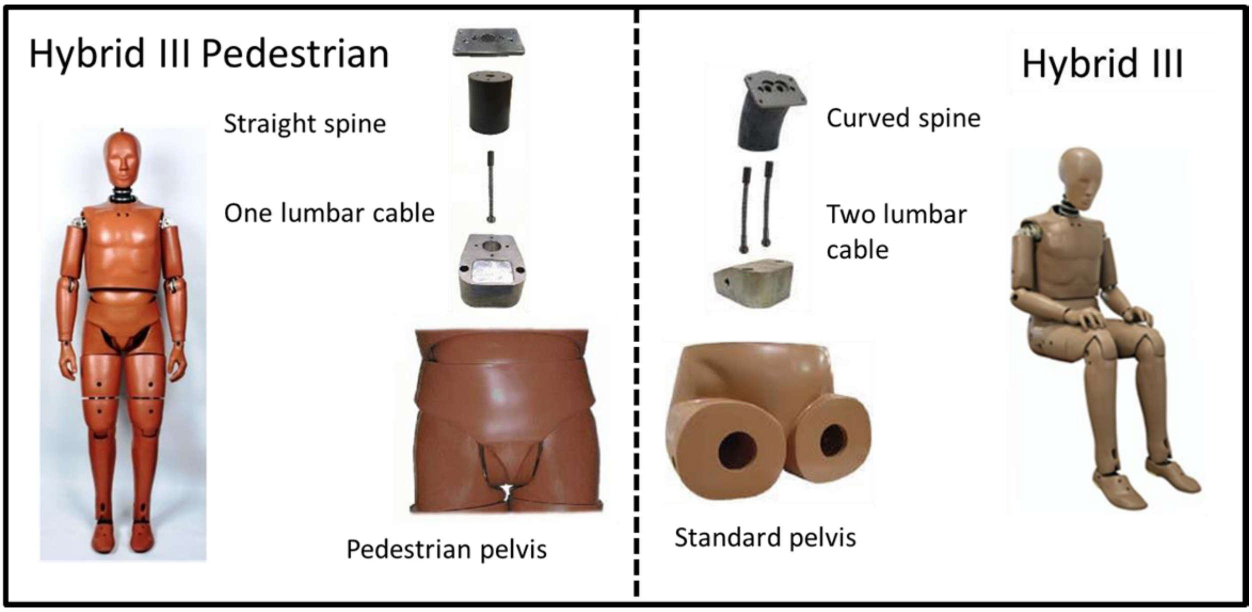

Figure 1. Pelvis flesh and lumbar joint differences between the Hybrid III Pedestrian ATD (left) and Hybrid III ATD (right)

Optoelectronic stereophotogrammetric system: ATD and buck kinematics data were captured at 500 Hz with a 26 camera optoelectronic stereophotogrammetric system (OSS) (Vicon MX, Vicon, Los Angeles, CA) (Figure 3). The motion capture system tracked the trajectories of spherical retroreflective markers through a calibrated 3D space within the cameras' collective field of view. Markers were secured to the head, spine, shoulders and pelvis of each ATD. Additional markers were attached to the restraints and rigid structure of the vehicle buck. Using a methodology reported in detail previously [11-12], rigid body mechanics were applied to determine ATD kinematics with respect to the local vehicle coordinate system using coordinate transformation. Four anatomical locations were selected to quantify excursion for each ATD. These locations were the head, T1 (top of thorax), T8 (middle of thorax) and pelvis. Multiple markers secured to the head provided head CG excursion. A four-marker array secured to the ATD upper spine was used to provide excursions of T1 and T8 using the method described in detail by Parent et al. [13]. A single marker secured to the posterior aspect of the pelvis provided excursion of the pelvis. Additionally, one on-board high speed video camera was used to visualize ATD motions at 50 Hz (quasi-static) or 500 Hz (dynamic) (HR-CAM,GX-5, NAC Image Technology, Simi Valley, CA).

Test Procedure

With the ATDs and other equipment installed on the buck, it was balanced following the procedure described by Kerrigan et al. [14] to ensure the rotation axis of the buck passed through the CG of the buck. Each ATD was positioned prior to the test in a manner that closely approximated that of the UMTRI standard driving position [15] commonly utilized in frontal and side impact testing with both ATDs and PMHS [11, 16]. The midline of each ATD was aligned with the seat centreline. The ATD chest was pitched rearward until the head's position had a zero (+/- 2 degrees) degree flexion angle relative to the floor. This resulted in a sternum angle of approximately 69 degrees (from horizontal). Then the ATD was pushed rearward, maintaining the angle of the chest and head, until the upper seat blocks contacted the ATD's back (Table 1 and Figure 2). Then the feet were placed on the toe pan and the thigh and leg sections were oriented to 15 and 46 degrees with respect to the horizontal, respectively. The belt was buckled around the ATD, and the shoulder and lap belt were tightened (via turnbuckles) until the belt load cells each registered 35 N, and the belt position was measured (Table 1). The ATD hands were strapped to the thighs to prevent interaction between the two dummies and ensure that upper extremity motion would not impede motion tracking. Due to the differences in the lumbar and knee joints, the H3P had a greater seated height and slightly different lower extremity positions.

Table 1. Positioning and belt measurements averaged over all eight tests.

		H3		H3P	
		Avg.	**SD**	**Avg.**	**SD**
Uny	Lateral distance from the upper neck center to the door interior (mm)	300	0.9	299.6	1.8
Scy	lateral distance from sternum center to door interior (mm)	298.5	2	302.4	1.6
SA	Thorax (sternum) angle (degrees)	69	0.5	69	0
Hax	Head Flexion/Extension (degrees)	1.2	0.6	1	0.5
Hay	Head Lateral Bending (degrees)	0.9	0.6	1	0.6
SHz	Seated Height (mm)	840	5	873	7.6
FA	Femur Angle (degrees)	15	0.4	15.4	0.5
TA	Tibia Angle (degrees)	44.2	12.1	48.3	0.5
Kcy-in	Lateral distance from the knee center to the door interior-inboard (mm)	416.5	5.8	468	15.3
Kcy-out	Lateral distance from the knee center to the door interior-outboard (mm)	178.6	7.2	127.9	13.2
SB	Shoulder Belt Load (N)	34	3	33.9	2.4
LB	Lap Belt Load (N)	36	2.5	32.9	2.2
A	Neck outer at CL to inner belt edge	28.5	1.2	30.3	2.4
B	Inner belt edge from centerline at top of jacket holes (mm)	18.4	0.9	23.6	1.4
C	Inner belt edge from centerline at sternum (mm)	62.6	8.1	57.3	1.6
D	Lower belt edge to sternum mark on centerline (mm)	89.6	1.3	79.8	1.8
E	Upper belt edge to sternum mark on centerline (mm)	170.4	1.5	164.4	0.9
F	Angle of belt from horizontal (degrees)	54.9	1.8	56.3	1.7
G	Belt angle to shoulder from horizontal (degrees)	21.5	1.3	16.6	1.4
H	Belt stock turnbuckle angle (degrees)	51.6	1.6	52	2

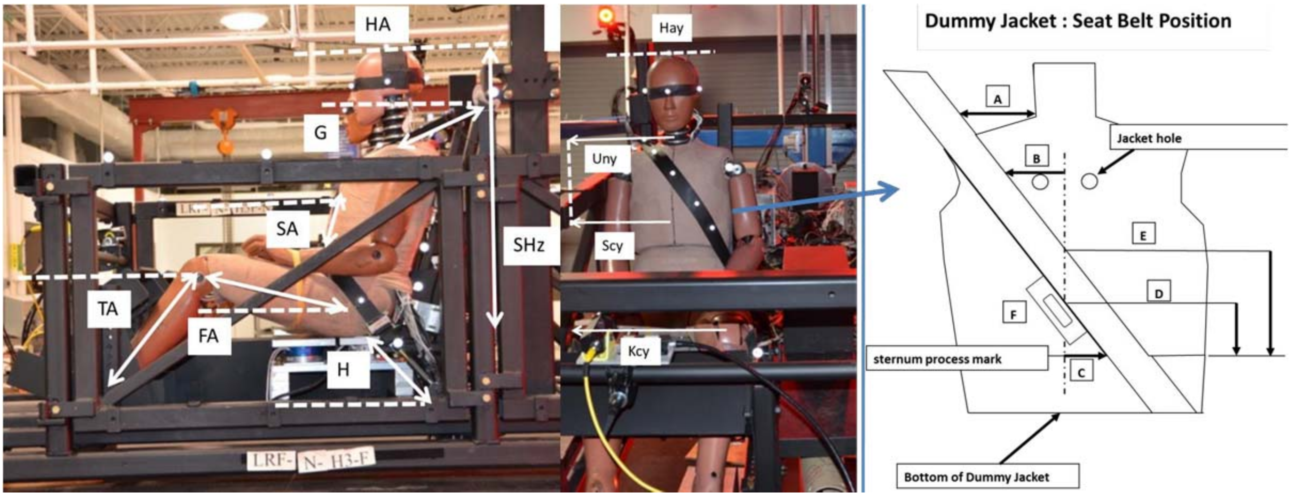

Figure 2. Positioned ATD: side view and front view

Test Condition: Initially, the buck was oriented upright (0 degree roll angle) with a 5 degree negative pitch (front end down) (Figure 3). Three different types of passenger side leading tests were performed:

Quasi-Static roll test (QR): The buck was manually rotated at a relatively constant roll rate to a roll angle of 180 degrees in approximately 20 seconds.

Dynamic roll test: The DRoTS roll drive rotated the buck one revolution (360 degrees) over three different phases: Phase 1-relatively constant angular acceleration over roll angles from 0 to 125 degrees; Phase 2-relatively constant angular velocity over roll angles 125 to 235 degrees; Phase 3-relatively constant angular deceleration to a complete stop over roll angles from 235 to 360 degrees. The Phase 2 average velocity was 180 deg/s in the low-rate (LR) test, and 360 deg/s in the high-rate (HR) test.

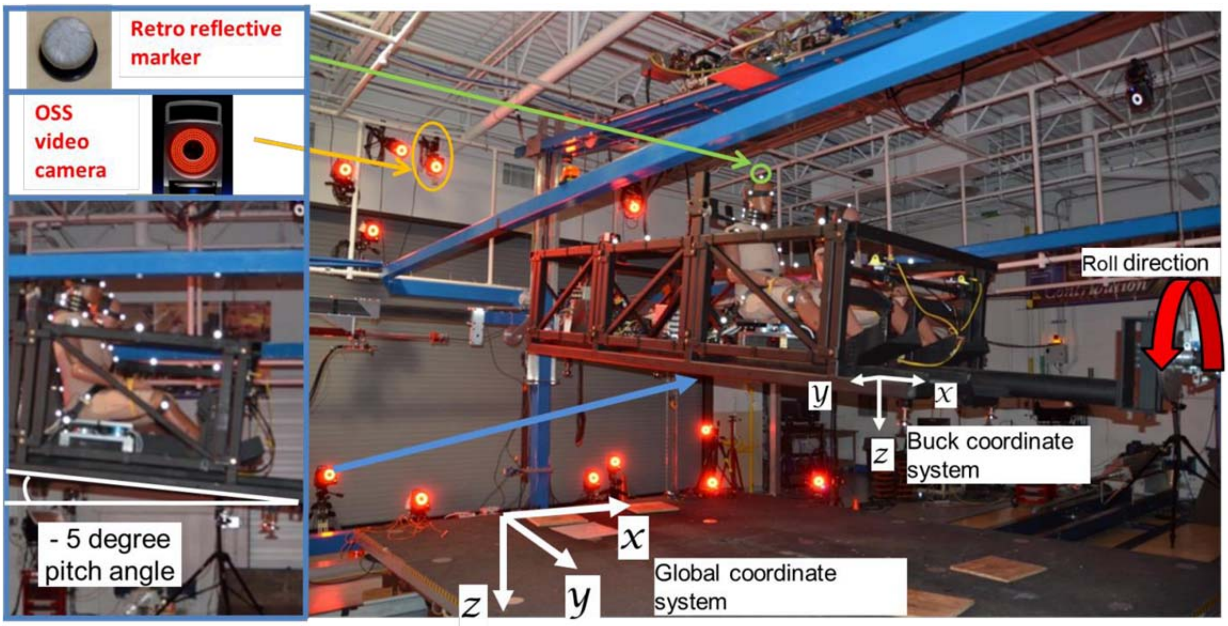

Figure 3. DRoTS rollover buck testing system overview

ATD test condition: Each ATD was tested in each of the three test conditions, in each of the two (leading and trailing side) seats (Table 2). To evaluate repeatability additional HR tests were performed for each ATD in each seating position.

Table 2. Test matrix (eight tests in total)

H3 Trailing, H3P Leading				
Test condition	QR	LR	HR	
Test Number	1849QR	1850LR	1848HR	1858HR
H3P Trailing, H3 Leading				
Test condition	QR	LR	HR	
Test Number	1860QR	1861LR	1862HR	1863HR

Data Processing

Buck and ATD sensor data were debiased and filtered using standardized criteria [17]. The data collected from the motion capture system were combined with a rigid body motion analysis that yielded three dimensional position time histories of the head, T1, T8 and pelvis relative to the local (buck) coordinate system. The Y and Z excursions of the ATD segments, defined as maximum upward vertical (Z) and outboard lateral (Y) displacement, were calculated from the position time histories. The ATD's lean angle, *LeanAngle* = $\arctan[(Y_{T1}-Y_{Pelvis})/(Z_{T1}-Z_{Pelvis})]$, was calculated to characterize the ATD's lateral orientation relative to the buck. The pitch angle of the ATD segments (Head-T1, T1-T8, T8-Pelvis) were also defined as $P = \arctan[(X_{Head}-X_{T1})/(Z_{Head}-Z_{T1})]$, $P_{Thorax}= \arctan[(X_{T1}-X_{T8})/(Z_{T1}-Z_{T8})]$, $P_{Pelvis} = \arctan[(X_{T8}-X_{Pelvis})/(Z_{T8}-Z_{Pelvis})]$ respectively to characterize the ATD`s sagittal rotation motion relative to the buck.

To provide for a quantitative assessment of dummy response repeatability (in HR tests), a signal correlation analysis was performed to compare the time histories of ATD position [18-21]. The correlation methodology assigns three values to each pair of curves compared: (1) a magnitude coefficient, which has a value of 1.0 for identical magnitudes and values less than 1.0 representing one signal's magnitude as a percentage of the other; (2) a shape coefficient, which does not have units and can have values between 1 (same shape) and 0 (no correlation); and lastly (3) a phase shift, which is expressed in units of time, describing the phase shift between two signals.

III. RESULTS

Test repeatability

The repeatability of the test method was evaluated by comparing the buck CG kinematics of the QR, LR and HR tests, and ATD head, T1, T8 and pelvis position time histories in the HR tests. While there was some variation due to manual rotation in the QR tests, the LR and HR tests showed almost identical roll angle and roll rate time histories (Appendix Figure A3). Both the H3 and H3P showed very repeatable kinematics (Figure A4-A7). The kinematics of the ATD head, T1, T8 and pelvis showed that while initial positions were not identical, position time histories from different tests converged usually within the first 500 ms (e.g. Figure A4 Head Z). This indicated that ATD kinematics were not sensitive to small variations in ATD initial position. The ATD response repeatability was also evaluated by the signal correlation analysis (Tables A1). The kinematics data showed very high similarity in repeated tests (on average, magnitude: >0.95, shape: 1.000, phase: <16 ms).

ATD kinematics

During the tests, both ATDs generally drifted outboard (laterally) and upward, and the upper body pitched forward, causing the head to move forward from the seat and the pelvis to move backward toward the seat. ATD position vs buck roll angle histories were compared to evaluate differences between dummies from the QR (Figures A8 and A9), LR (Figures A10 and A11) and HR (Figures A12 and A13) tests. In addition, the ATD LeanAngle vs buck roll angle histories was also shown in Figure A14. In general, ATD kinematics varied by roll rates and seating position.

Quasi-static tests: During the initial stage of rotation (roll angle 0-60 degrees), both dummies leaned rightward (inboard for the trailing-side ATD, outboard for the leading-side ATD) gradually due to the gravity (Figure 4, Figure A14). The dummies did not slide to the right, however, due to friction between the ATD pelvis and the seat pan. During this period, the majority of the outboard lateral excursion that occurred in this test took place. During the next stage (60-110 degrees), no significant motions of the dummies were observed. Starting around 110 degrees for the trailing-side and 150 degrees for the leading-side, the ATD lost contact with the seat due to gravity and underwent vertical excursion.

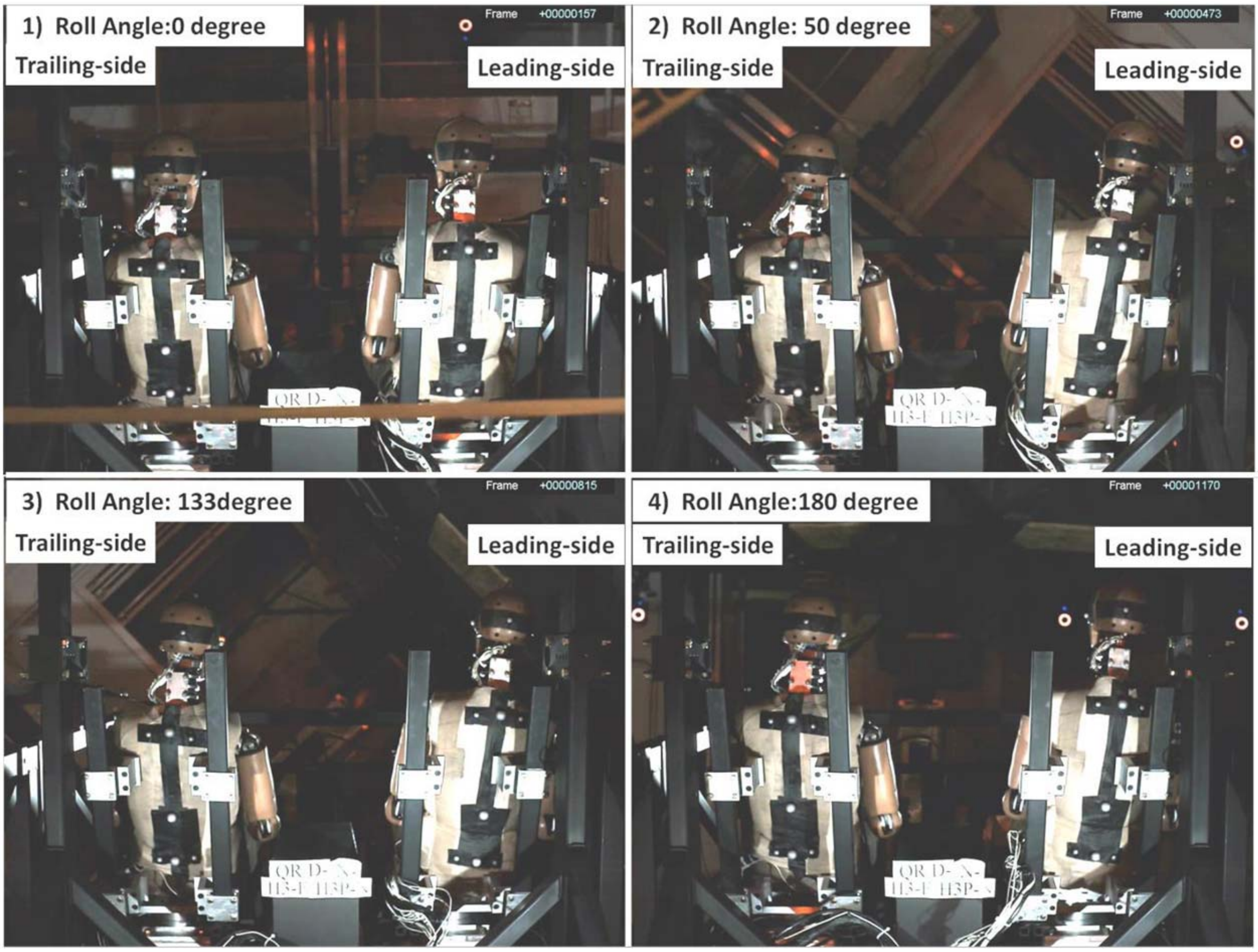

Figure 4. ATD kinematics in QR tests: H3 (left) is the trailing occupant and H3P (right) is the leading occupant (Test 1849QR).

Low roll rate tests: During the initial stage of Phase 1 (roll angles of 0-125 degrees), the leading-side ATD leaned outboard first, quickly followed by the pelvis sliding outboard (Figure 5, Figure A14). By 80 degrees of rotation the trailing-side ATD had moved slightly inboard and upward. Then between 100-125 degrees, the pelvis of the trailing-side ATD slid inboard, which resulted in an outboard lean angle. Then during Phase 2 (125-235 degrees) the pelvis of the trailing-side ATD started to slide back outboard, which eliminated the lean angle, because the roll rate during this period was a maximum (and thus the upward and outboard directed centrifugal force was maximized), and the pelvis was no longer in contact with the seat. In addition, due to the buck orientation during this period, the effect of gravity on the ATD`s lateral motion was small, whereas the ATD vertical motion was dictated by a combination of gravity and centrifugal force. Additionally as the ATD moved upwards, the ATD`s pelvis moved backward while the head moved forward, which resulted in a forward pitching rotation. During Phase 3 (235-360 degrees) both ATDs` pelves slid to the left, which resulted in rightward lean angle until the buck’s rotational motion ended. During this period, the buck was decelerating, which caused the ATDs to lean rightwards due to inertia while gravity pulled the ATDs’ pelves leftwards.

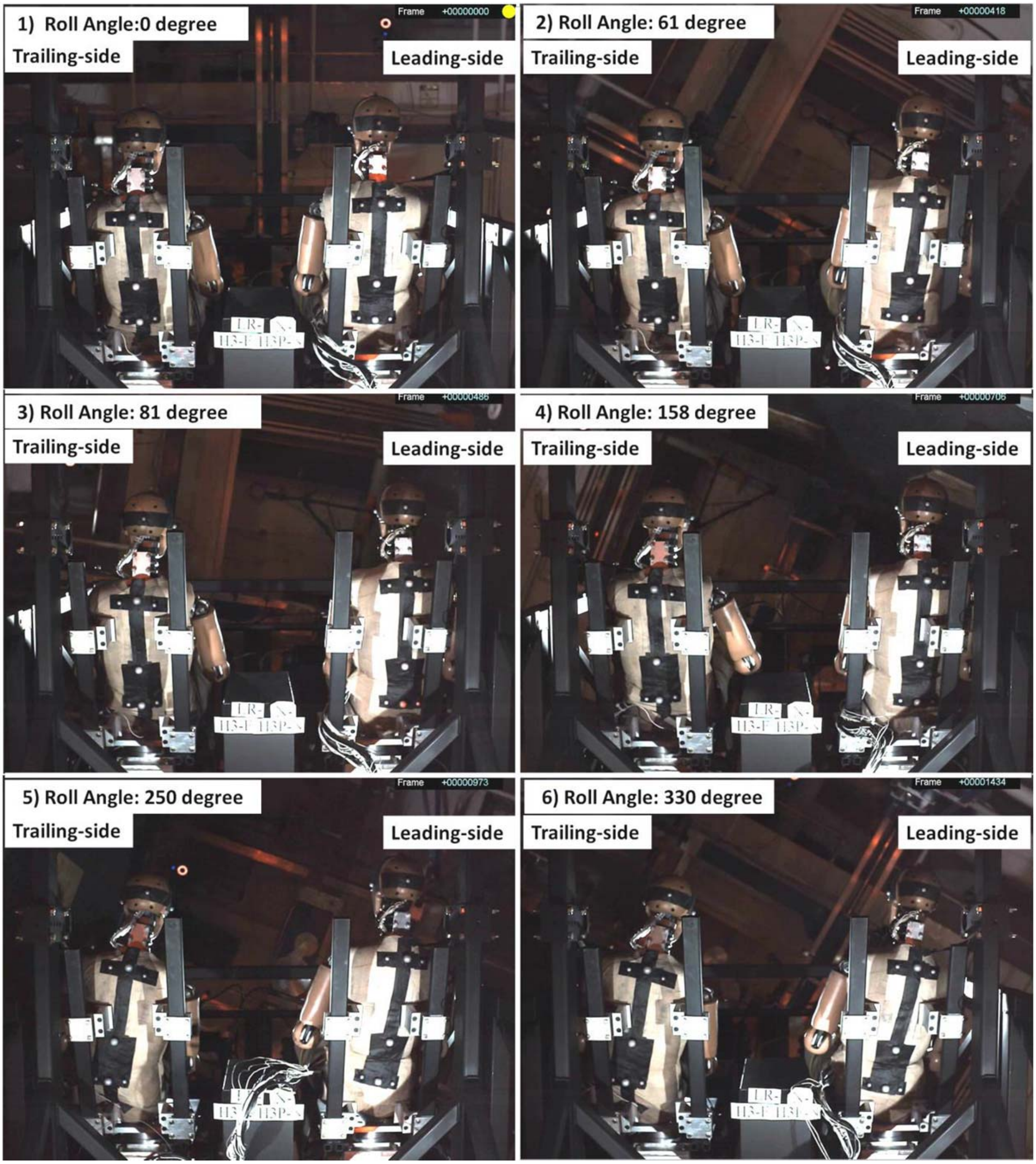

Figure 5. ATD kinematics in LR tests: H3 (left) is the trailing occupant and H3P (right) is the leading occupant (Test 1850).

High roll rate tests: During the initial stage of Phase 1, due to inertia, the upper body of the trailing-side ATD moved outboard slightly, which resulted in an outboard lean angle, while the upper body of the leading-side ATD moved inboard slightly, which resulted in an inboard lean angle (Figure 6 and Figure A14). Starting at around 50 degrees, as the pelvis came off the seat due to the centrifugal force, the leading-side ATD`s pelvis began to move outboard before the upper torso, which resulted in an inboard lean. However, this lean angle quickly decreased when the upper body of the ATD moved outboard due to the centrifugal force and gravity. Then the trailing-side ATD started to move outboard and upward at a roll angle around 80 degrees (both the thorax and the pelvis moved outboard at relatively the same time). The trailing-side ATD moved outboard after the leading-side ATD, mainly because gravity helped to pull the near side ATD outboard while it counteracted the outboard motion of the trailing-side ATD. At the same time as both dummies were moving upwards, the pelves also moved backwards and the head moved forward causing a forward pitch of the thorax. In Phase 2, both the trailing- and leading-side dummies remained outboard and upward with relatively little motion. In Phase 3, the leading-side ATD started to lean inboard and move downward (back to the seat) at around 300 degrees roll angle. This was mainly because the centrifugal forces decreased as the roll rate decreased and the relative contribution of gravity increased, which brought the ATD back down to the seat at a location farther outboard than it started. The trailing-side ATD leaned inboard at the end of the tests due to its inertia during the buck deceleration.

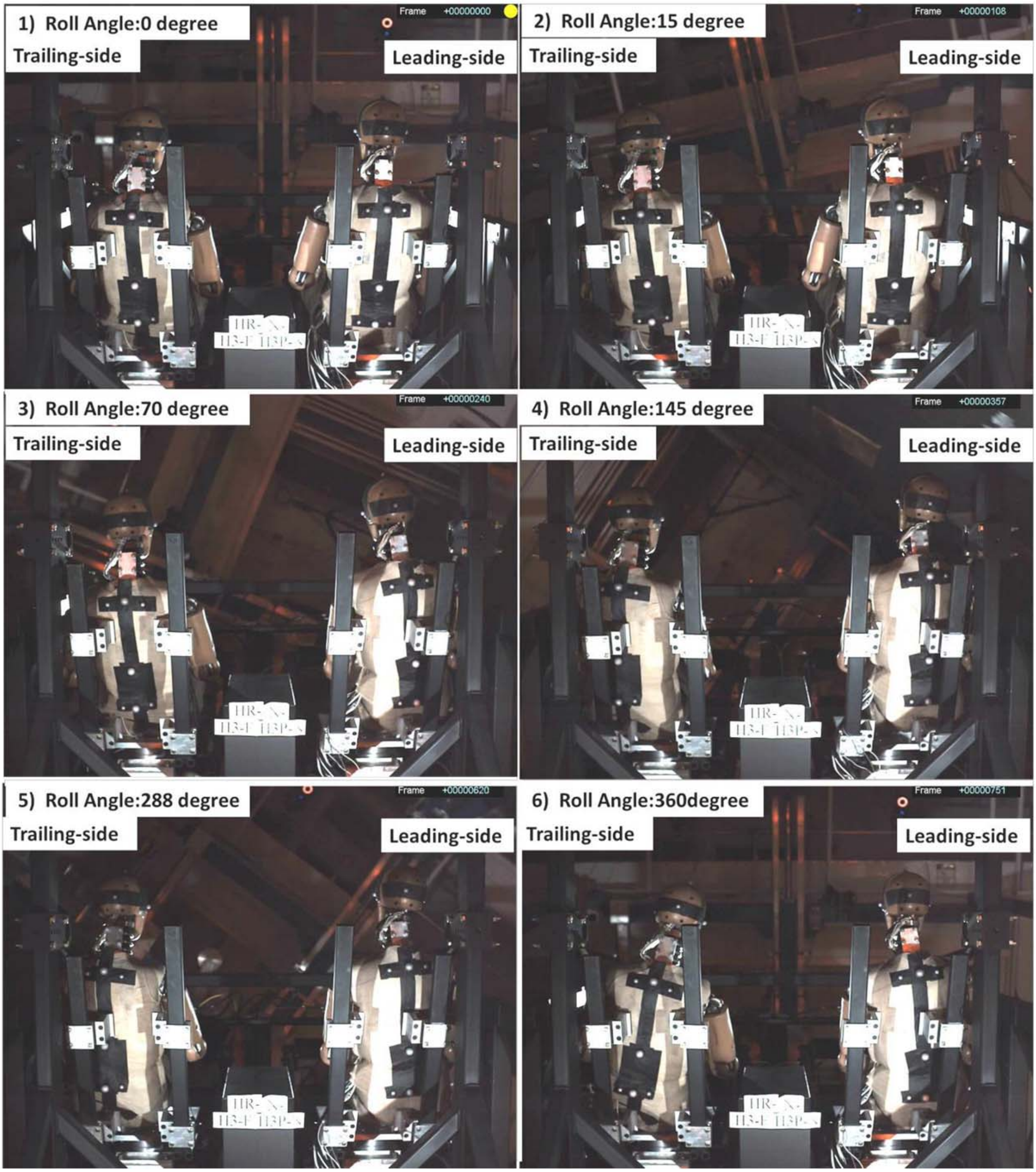

Figure 6. ATD kinematics in HR tests: H3 (left) is the trailing occupant and H3P (right) is the leading occupant (Test 1848).

ATD vertical, lateral excursion and pitch rotation motion

During the tests, both ATDs generally drifted outboard (laterally) and upward, and the upper body pitched forward, causing the head to move forward from the seat and the pelvis to move backward toward the seat. The occupant motion is quantified by the lateral excursion, vertical excursion at head, T1, T8 and Pelvis, and pitch rotations of the Head-T1, T1-T8 and T8-Pelvis segments in this study.

The vertical and lateral excursions of the head, T1, T8 and Pelvis were calculated for both ATDs from each test (Appendix Table A2). The vertical excursion ranged from 25mm (Pelvis of H3P ATD in trailing-side in QR test) to 88mm (T8 of H3 ATD in trailing-side in HR test). It was observed that the maximum vertical excursions increased as the roll rate increased (average 40mm for QR tests, 53mm for LR tests and 63 mm for HR tests); but not very sensitive to the seating position(average 52mm for trailing-side occupant and average 58mm for leading-side occupant). It was also observed consistently that the ATD`s head had less vertical excursions than the T1, the T1 had less vertical excursion than T8, and T8 had more vertical excursion than the ATD`s pelvis (Table A3). If the smaller motions of the more distal portion (eg. head) compared to a more proximal portion (eg.T1) as compression, and the opposite as tension, then in all of the HR tests, the neck was in "compression" (defined as HeadZ-T1Z), the thoracic spine was in "compression" (defined as T1Z-T8Z), and the lumbar spine was in "tension" (defined as T8Z-PelvisZ), as shown in the last three columns in Table A2.

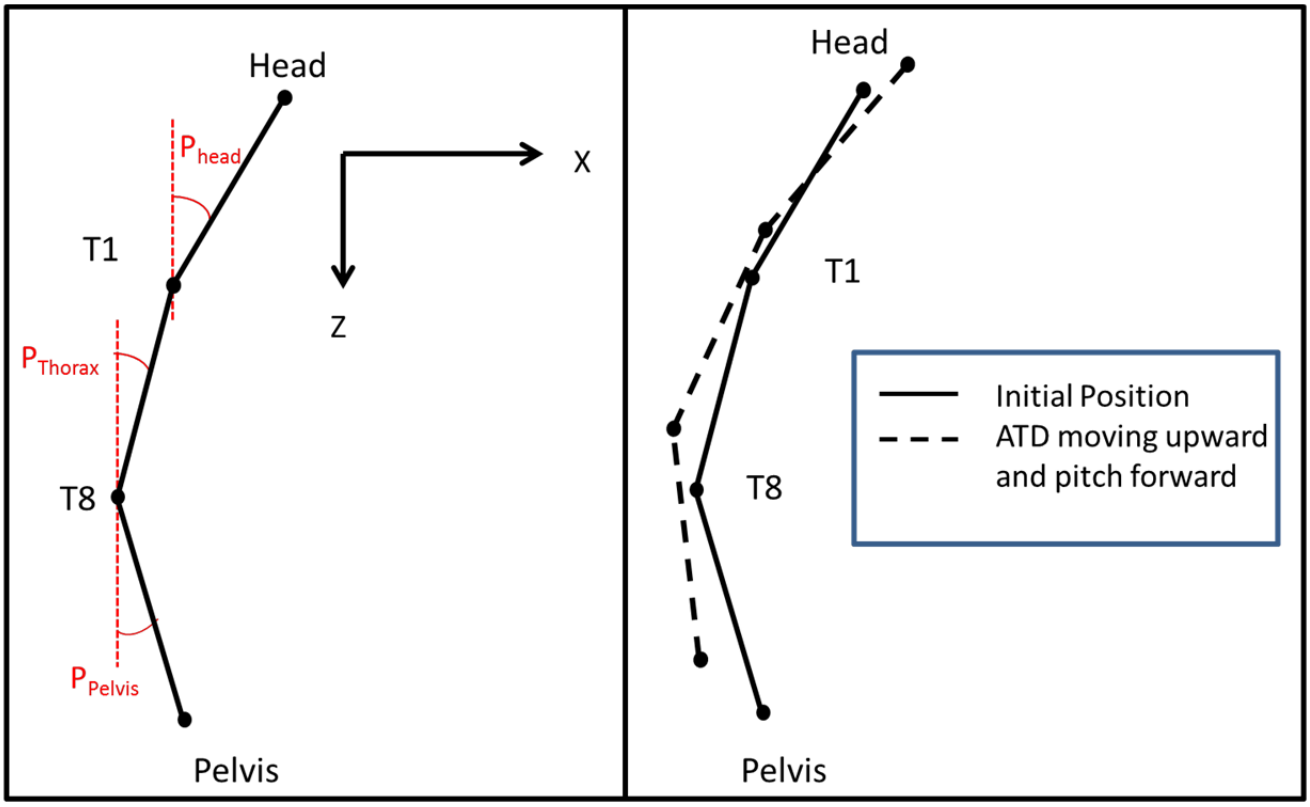

Figure 7. Lateral view of ATD pitch angle segments(Left)(the sign of pitch angle follow SAE convention, therefore P_{Head} and P_{Thorax} are positive while P_{Pelvis} is negative) and ATD motion(upward motion and pitch rotation) during the tests (Right).

However, further investigation on the ATD kinematics indicates that the apparent "compression" and "tension" observed above is because that as the ATD moved vertically upwards during the tests, the ATD also pitched forward (rotational motion). Initially, Head-T1 segment pitched forward at pitch angle around -23 to -25 degrees, T1-T8 segment pitched forward at pitch angle around -12 to -15 degrees, and T8-Pelvis segment pitched backwards at pitch angle around 14 to 16 degrees (Figure 7 Left). During the tests, the ATD pitched forward as the ATD moved vertically upward, which caused the Head-T1 and T1-T8 segment more horizontal while T8-Pelvis segment more vertical. These resulted in the apparent "compression" for the Head-T1 and T1-T8 segment, and "tension" for the T8-Pelvis segment. The pitch rotation of the Head-T1, T1-T8 and T8-Pelvis segments VS buck roll angle was shown in Figure A15, A16 and A17 respectively (initial pitch angle was shifted to be 0 degree to facilitate comparison). In general, the ATDs pitched around 4-6 degrees forward in QR tests and 8-12 degrees forward in LR and HR tests. In addition, this pitch motion also resulted in the forward motion of the head and backward motion of the pelvis towards the seat (Figure A8, A9, A10, A11, A12 and A13).

To account for the ATD out-of-plane motion and thus more accurately characterize the compression and tension state of the ATD segments, the resultant distances of the ATD segments (Head-T1, T1-T8 and T8-Pelvis) were calculated based on the OSS three-dimension kinematic data. It was observed that the Head-T1 distance oscillated (within 10mm range), which might mainly be due to the flexion/extension bending of the ATD neck. The T1-T8 distance remained constant at 152mm. The T8-Pelvis distance increased slightly (10mm or less) during the tests, which might be due to the straightening of the pelvis and thorax.

The lateral excursion ranged from 0mm (head of H3P in trailing-side in QR test) to 139mm (pelvis of H3P in leading-side in HR test). For leading-side occupant, the lateral head excursion decreased as the roll rate increased, while the pelvis excursion increased as roll rate increased. For the trailing-side occupant, head lateral excursions increased as roll rate increased, and pelvis lateral excursions were largest in the LR tests.

It was also observed that for the leading-side occupant, the maximum lateral excursion decreased from ATD head to pelvis in QR and LR tests (eg. in QR test, at leading-side, H3 ATD has lateral excursion 99mm at Head, 74mm at T1, 61mm at T8 and 43mm at Pelvis), but increased from ATD head to pelvis in HR tests. However, for the trailing-side occupant, the maximum lateral excursion increased from ATD head to pelvis in QR and LR tests, but decreased in HR tests (Table A2). This is because, in QR and LR tests, the ATDs tended to lean inboard at the trailing-side position, outboard at the leading-side position. In HR tests, the ATDs tended to lean outboard at the trailing-side position, inboard at the leading-side position (Figure A14).

The differences of the maximum lateral and vertical excursions between the H3 and H3P ATDs were also reported in Table A3. In general, the H3 ATD had larger vertical excursions and smaller lateral excursions than the H3P, except that for the T8 and Pelvis lateral excursions in trailing-side in the HR tests, the H3 had more lateral excursions than the H3P.

IV. DISCUSSION

This study is part of a larger study aimed at evaluating the biofidelity of existing ATDs in rollover crash-like loading. Although the rollover buck was designed to mimic a full-sized SUV in the US market, it is not the purpose of this study to determine the occupant excursion in real-world rollover crashes, as several simplifications were made in terms of both the vehicle and test conditions to ensure a more controlled and repeatable test methodology. A simplified vehicle test buck, including simplified rigid seats and other interior components, was used as the test vehicle and pure rotations about the simulated center of gravity were performed. The goal of these tests was to impart centrifugal accelerations to crash ATDs restrained with 3-point seat belts, and perform detailed measurements of their kinematic response to use in comparing responses between ATDs and post mortem human surrogates (PMHS). The simplified buck with simplified structures was chosen to facilitate computational modeling, parametric analysis, optical motion tracking, and to ensure that buck tests could be easily repeated in the future. The pure roll condition simulates the ballistic phase of a rollover when vehicles rotate about their CGs. However, because the buck was not actually airborne during the tests, the occupants were subjected to gravitational accelerations in addition to the centrifugal accelerations resulting from the buck rotation. In rollover crashes, when the vehicle goes ballistic, the centrifugal accelerations cause the occupants to move out of position and away from the vehicle's CG. The occupant position and orientation relative to the vehicle roof and pillar structures will affect injury risk when the vehicle impacts the ground since the loading direction has been shown to affect injury risk [22]. Thus, the goal of the study was to describe ATD three-dimensional kinematic responses under such accelerations and compare responses between the H3 and the H3P ATD.

Overall, there were three different factors that influenced ATD motion and excursion: 1) *centrifugal acceleration*: from the buck's rotational motion that caused each ATD to move outboard and upward (For a mass 1 m away from the center of rotation, at 180 deg/s and 360 deg/s, centrifugal accelerations are approximately 1 g and 4 g respectively); 2) *gravity:* that pulled the ATD upward, downward and laterally, depending on the direction of the gravity vector relative to the buck; and 3) *inertia*: the ATD leaned leftward and rightward relative to the buck when the buck accelerated and decelerated, respectively.

In QR tests, the ATD motion was dominated by gravity, as the centrifugal force and the inertial forces were negligible due to the low rotation rate. Gravity caused the ATDs to move laterally in Phase 1 and vertically (out of the seat) in Phase 2 (Figure 4, A8 and A9). In LR tests, the centrifugal force, gravity and inertia all had substantial effects on ATD kinematics causing lateral and vertical motions to vary across the three phases (Figure 5, A10 and A11). In HR tests, the ATDs in both seating positions moved upward and outboard due to the centrifugal force and remained (generally) stationary until near the end of deceleration (Figure 6, A12 and A13). For the LR and HR tests, maximum lateral excursions typically occurred in Phase 1 or 3, while maximum vertical excursions occurred in Phase 2. During Phases 1 and 3, while the buck was generally oriented on its side with gravity directed laterally with respect to the seat, and angular velocities were relatively low, gravity and inertia dominated ATD kinematics causing the dummies to move laterally. During Phase 2, when the buck was generally oriented upside down and rotation rates were maximized, gravitational acceleration and centrifugal accelerations pulled the ATD moving vertically upward.

Effect of roll rate and seating position on ATD excursion

Due to the difference in centrifugal accelerations seen by the ATDs in the three tests, ATD response varied as a function of roll rate. Additionally, since the buck only rotated 360 degrees, a steady state condition like that previously described by Moffat et al [6] was not achieved and, as a result, there were differences in ATD response based on seating position compared to Moffat`s study. In particular, maximum vertical and lateral excursions, which generally occurred in different phases of the event, varied as a function of roll rate and seating position.

Vertical Excursion: The maximum vertical excursion typically occurred in phase 2.

• Effect of roll rate: in general, as the roll rate increased, the maximum vertical excursion increased consistently due to the increased acceleration applied on the ATDs.

• Effect of seating position: the seating position affected the ATD motion through the gravity vector direction relative to the ATD. As maximum vertical excursion typically happened in phase 2, the effect of seating position on the vertical excursion was not significant, as during phase 2, the gravity vector aligned symmetrically between the trailing-side and leading-side occupant. Moffatt et al. [6] conducted a series of pure roll tests on dummies and human volunteers, and found that while the head excursion was similar between trailing-side and leading-side occupant in the static roll tests, in the dynamic roll tests, the trailing-side occupant has much larger head vertical excursion than the leading-side occupant. As the authors mentioned, the outboard shoulder of the trailing-side occupant in their tests tended to slip out from the shoulder belt when he leaned inboard away from the shoulder belt, and therefore the trailing-side ATD tends to have more vertical excursion. This phenomenon did not happen in our tests. This is because the DRoTS system spun the rollover buck to the desired roll rate within 125 degrees, while the roll fixture used by Moffat et al. spun the vehicle up to the desired roll rate in about three revolutions. Therefore, our test fixture achieved the target roll rate much faster and the trailing-side ATD did not slip out of the shoulder due to gravity.

Lateral excursion: The maximum lateral excursion typically occurred in phase 1 or 3.

• *Effect of roll rate*: as the roll rate increased, the ATD as a whole moved more laterally outboard. However, when considering a specific body region (head, T1, T8, pelvis), no consistent trend was observed. The effects of gravity and inertia should be considered, as the ATD tends to lean laterally during LR tests (Figure 5), which resulted in a large upper body lateral excursion but small lower body (pelvis) lateral excursion, and thus complicate the effects of roll rate on ATD lateral excursion.

– *Leading-side occupant*: the maximum lateral excursion occurred in phase 1. In general, the lower the roll rate, the more the lateral excursion is dictated by the gravity. Gravity caused the ATD to lean laterally. The occupant leaned outboard the most in quasi-static tests (8 degree), followed by the lower rate tests (5 degree), and in the high rate tests, the ATD actually leaned inboard (-3 degree). Therefore, for the upper body (head), the lateral excursion decreased as roll rate increased, while for the lower body (pelvis), the lateral excursion increased as roll rate increased.

– *Trailing-side occupant*: the maximum lateral outboard excursion occurred in phase 1 for the HR tests, in phase 3 for the LR tests, for the QR tests, almost no outboard lateral excursion as gravity tended to pull the ATD inboard laterally. For phase 3 of the LR tests, the ATD leaned inboard due to the inertia force from the buck deceleration. At the same time the gravity also pulled the ATD outboard laterally. But for the HR tests, the ATD moved outboard without much lean angle. Therefore the upper body excursions increased as roll rate increased from LR to HR; while the lower body excursion in LR was comparable or even larger than the HR tests.

- *Effect of seating position*: the lateral excursions were different between leading-side and trailing-side occupants.

– For the QR tests, the leading-side ATD had larger lateral excursion than the trailing-side occupant. This occurred because in phase 1, the gravity pulled the leading-side ATD outboard but the trailing-side ATD inboard.

– For the LR tests, the maximum lateral excursion of leading-side ATD occurred in phase 1 with an outboard lean (due to gravity), while the maximum lateral excursion of trailing-side ATD occurred in phase 3 with an inboard lean (due to inertia from buck deceleration). Therefore, the leading-side ATD had less lateral excursion at the pelvis, but more lateral excursion at the head compared to the trailing-side ATD.

– For the HR tests, the effects of seating position on lateral excursion of the two ATDs were different. For H3 ATD, the difference of lateral excursion was not as great as in the QR and LR tests, since in the HR tests, the centrifugal acceleration was very large and tended to dictate the ATD excursion. For H3P ATD, however, it seemed that the H3P ATD exhibited smaller pelvis excursion but larger head excursion in the trailing-side seating position than in the leading-side seating position (Table A2, A3). This is because H3P ATD in trailing-side position leaned outboard significantly due to the inertia from the buck acceleration, while H3P ATD in the leading-side position actually leaned inboard slightly (Figure 8, and Figure A14).

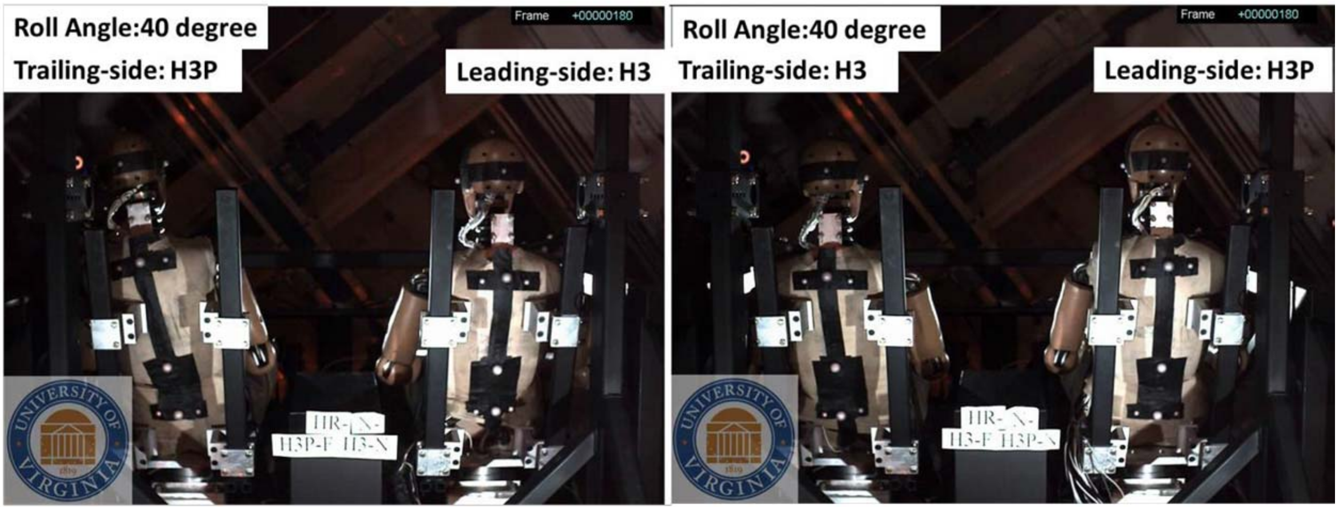

Figure 8. H3P VS H3 ATD in the trailing-side and leading-side position in HR tests

The kinematic differences between Hybrid III and Hybrid III Pedestrian ATD

Vertical excursion and forward pitch motion: For both ATDs, the upward vertical motion was accompanied with the pelvis moving backward and the upper body moving forward, resulting in a forward pitch rotation. The H3P ATD had less vertical excursions compared with the H3 ATD consistently (Appendix Table A2, A3). In addition, the pitch rotation angles were also less significant in the H3P ATD than in the H3 ATD (Appendix Table A4). These two differences (vertical excursion and pitch rotation) may be due to the increased mobility of the hip joint in the H3P ATD (unmolded pelvis flesh). The increased mobility of the hip joint in H3P ATD resulted in larger upward motion (with respect to buck) of the lower extremity by flexion of the hip joint, which limited the ability of centrifugal acceleration to pull the H3P ATD upward through the torso. Therefore, the H3 ATD achieved a larger vertical excursion and a slightly more forward pitch rotation. The increased mobility of the hip joint in the H3P ATD might better simulate the occupant response in the rollover crashes.

Lateral excursion: H3P ATD in general had more lateral excursion across all of the current test conditions, except in the trailing-side seating position in the HR tests. In this condition, the H3P ATD had much more head lateral excursion, but much less pelvis lateral excursion. The H3P ATD had only one lumbar cable in the center of the lumbar spine while the H3 ATD had two lumbar cables there (Figure 1). Therefore, decreased lumbar spine stiffness in lateral bending of the H3P ATD was expected. Therefore, greater lateral excursion of the H3P ATD might be because 1) both the head, upper thorax and the pelvis could bend more outboard by the bending of the lumbar joint in the H3P ATD, 2) the H3P ATD is around 35 mm taller than the H3 ATD, which can permit the dummy to undergo more lateral excursion when bending the lumbar joint laterally. However, during the HR tests in the trailing-side seating position, the relative lateral bending between the thorax and the pelvis was so significant in the H3P ATD (Figure 8), that the upper body (head and upper thorax) of the H3P ATD moved outboard and upward, which resulted in an apparent outboard lean angle (Appendix Figure A14). Therefore, the H3P ATD had much larger head lateral excursion but much smaller pelvis lateral excursions compared with the H3 ATD in this test condition (HR tests, trailing-side seating position). The H3 ATD was originally designed for frontal impact, and therefore the lack of the biofidelity in the lateral direction (eg. very high lateral stiffness) limits its use in the rollover crashes, since lateral loading is hypothesized to be one of the loading mechanisms in rollover crashes. The H3P ATD might behave closer to a PMHS in rollover crashes than H3 ATD due to the decreased lateral stiffness afforded by the single lumbar cable design.

V. CONCLUSIONS

This study presented a repeatable methodology using a vehicle-like parametric buck for studying the occupant kinematics in controlled laboratory tests aimed at simulating rollover crash vehicle kinematics. The occupants (H3 and H3P) moved in a three-dimensional fashion and their motions were affected by a combination of inertia, centrifugal acceleration and gravity during pure roll tests. The H3 and H3P kinematics were compared at different roll rates and seating positions. The H3P ATD repeatedly exhibited less vertical excursion and smaller forward pitch motion than the H3 ATD due to the increased mobility in the hip joint. In addition, the H3P ATD exhibited more lateral excursion compared with the H3 ATD due to the more compliance in lateral bending of the lumbar spines. The increased compliance of the lumbar spine and hip joints of the H3P ATD suggests that it may be more biofidelic in rollover crash testing than the H3 ATD; however, direct comparison to human response is needed before a biofidelity assessment can be complete. Such a comparison is a future goal of this ongoing research effort.

VI. ACKNOWLEDGEMENT

This study was supported by the National Highway Traffic Safety Administration (NHTSA) under Cooperative Agreement No. DTNH22-09-H-00247. Views or opinions expressed or implied are those of the authors and are not necessarily representative of the views or opinions of the NHTSA.

VII. REFERENCES

[1] National Highway Traffic Safety Administration (NHTSA). (2010) Traffic Safety Facts 2008—a compliation of motor vehicle crash data from the fatality analysis reporting system and the general estimate system. Early Edition. DOT HS 811 170. http://www-nrd.nhtsa.dot.gov/Pubs/811170.PDF

[2] Bahling G, Bundorf R, Kaspzyk G, Moffatt E, et al., Rollover and drop tests - The influence of roof strength on injury mechanics using belted dummies, SAE Technical Paper 902314, 1990, doi: 10.4271/902314.

[3] Moffatt E, Cooper E, Croteau J, Orlowski K, et al., Matched-pair rollover impacts of rollcaged and production roof cars using the controlled rollover impact system (CRIS), SAE Technical Paper 2003-01-0172, 2003, doi:10.4271/2003-01-0172.

[4] Bidez MW, Cochran JE, King D, Burke DS, Occupant dynamics in rollover crashes: influence of roof deformation and seat belt performance on probable spinal column injury, *Ann Biomed Eng,* 2007, 35(11):1973–1988.

[5] Raddin J, Cormier J, Smyth B, Croteau J, et al., Compressive neck injury and its relationship to head contact and torso motion during vehicle rollovers," *SAE Int. J. Passeng. Cars - Mech. Syst.* 2(1):914-941

[6] Moffatt E, Hare B, Iiyama H, Curzon A, et al, Head excursion of restrained human volunteers and Hybrid III dummies in steady state rollover tests, *47th Annual Proceedings of the AAAM*, September 22-24, 2003.

[7] Moffatt E, Cooper E, Croteau J, Parenteau C, et al., Head excursion of seat belted cadaver, volunteers and Hybrid III ATD in a dynamic/static rollover fixture," SAE Technical Paper 973347, 1997, doi: 10.4271/973347.

[8] Foltz P, Kim T, Kerrigan JR, Crandall JR, Vehicle greenhouse shape analysis for design of a parametric test buck for dynamic rollover testing, Paper Number 11-0271, *Proceedings of 22nd International Conference on the Enhanced Safety of Vehicles (ESV),* 2011.

[9] Toczyski J, Kerrigan JR, Mohan P, Crandall JR, Design of a deformable vehicle roof structure for rollover crash testing with a test buck, Paper 13-0203, *23rd International Conference on the Enhanced Safety of Vehicles (ESV),* Seoul, Korea, May 2013.

[10] Kerrigan JR, Jordan A, Parent D, Zhang Q, Funk J, Dennis NJ, Overby B, Bolton J, Crandall J, Design of a dynamic rollover test system, *Society of Automotive Engineers,* SAE Paper No. 2011-01-1116, 2011.

[11] Shaw G, et al., Impact response of restrained PMHS in frontal sled tests: Skeletal deformation patterns under seat belt loading, *Stapp Car Crash Journal,* 53:1-48, 2009.

[12] Lessley D, Shaw G, Riley P, Forman J, Crandall J (2011) Assessment and validation of a methodology for measuring anatomical kinematics of restrained occupants during motor vehicle collisions, *J Biosens Bioelectron* S1:002. doi: 10.4172/2155-6210.S1-002

[13] Parent D, Lessley D, Shaw G, Crandall J, Identification of anatomical landmarks for whole-body kinematic measurement in the THOR mod kit frontal impact ATD, *Japan Society of Automotive Engineers,* Paper No. 20125177.

[14]Kerrigan JR, Seppi J, Lockerby J, Foltz P, Overby B, Kim T, Dennis N, Crandall JR, Test methodology and initial results from a dynamic rollover test system, *Society of Automotive Engineers*, Paper No. 2013-01-0468.

[15] Schneider LW, Robbins DH, Pflug MA, Snyder RG, Anthropometry of Motor Vehicle Occupants, Vol. 3. Specifications and Drawings, Report HS-806 717, UMTRI-83-53-2, 1983.

[16] Lessley D, Shaw G, Parent D, Arregui-Dalmases C, Kindig M, Riley P, Purtsezov S, Sochor M, Gochenour T, Bolton J, Subit D, Crandall J, Takayama S, Ono K, Kamiji K, Yasuki T, Whole-body response to pure lateral impact, *Stapp Car Crash Journal*, 2010, 54:289-336.

[17]Society of Automotive Engineers (SAE), Inc., Instrumentation for Impact Tests. SAE J211/1 MAR95, March 1995.

[18]Xu L, Agaram V, Rouhana S, Hultman RW, Kostyniuk GW, McCleary J, Mertz H, Nusholtz GS, Scherer, R, Repeatability evaluation of the pre-prototype NHTSA advanced dummy compared to the Hybrid III," *Society of Automotive Engineers World Congress*, Detroit, MI, March 6-9, 2000, SAE Paper No. 2000-01-0165.

[19] Nusholtz GS, Hsu TP, Byers LC, A proposed side impact ATD bio-fidelity evaluation scheme using cross-correlation approach, Paper 07-0399. *Proceedings of the 20th International Conference on the Enhanced Safety of Vehicles (ESV), 2007,* http://www.nhtsa.gov/ESV.

[20] Gehre C, Gades H, Wernicke P. (2009) Objective rating of signals using test and simulation responses. Paper 09-0407, *Proceedings of the 21st International Conference on the Enhanced Safety of Vehicles (ESV),* http://www.nhtsa.gov/ESV

[21] Kerrigan JR, Dennis NJ, Parent DP, Purtsezov S, Ash JH, Crandall JR, Stein D, Test system, vehicle and occupant response repeatability evaluation in rollover crash tests: the deceleration rollover sled test, *International Journal of Crashworthiness*, 2 0 1 1 , 16(6): 583-605.

[22]Nightingale RW, McElhaney JH, Camacho DL, Kleinberger M, Winkelstein BA, Myers BS, The dynamic responses of the cervical spine: buckling, end conditions, and tolerance in compressive impacts, *Proceedings of the 41st Stapp Car Crash Conference*, 1997, pp. 451-71.

VIII. Appendix

Table A 1. Signal correlation analysis of the position time history response of H3 and H3P ATDs.

		Head X	Head Y	Head Z	T1X	T1Y	T1Z	T8X	T8Y	T8Z	Pelvis X	Pelvis Y	Pelvis Z	Average
H3-Far	Magnitude	0.974	0.998	0.991	0.994	0.996	0.997	0.968	0.993	0.991	0.958	0.986	0.945	0.982
	Shape	1.000	1.000	1.000	1.000	1.000	1.000	1.000	1.000	1.000	1.000	1.000	1.000	1.000
	Phase	-0.008	-0.004	-0.008	-0.012	-0.008	-0.006	0.004	-0.010	-0.002	0.000	0.000	-0.016	-0.006
H3-Near	Magnitude	0.956	0.968	0.991	0.974	0.963	0.984	0.992	0.968	0.976	0.954	0.984	0.958	0.972
	Shape	1.000	1.000	1.000	1.000	1.000	1.000	1.000	1.000	1.000	1.000	1.000	1.000	1.000
	Phase	-0.010	0.000	-0.004	0.010	-0.002	0.000	0.030	-0.002	0.000	0.000	0.000	0.000	0.002
H3P-Far	Magnitude	0.965	0.936	0.998	0.975	0.961	0.993	1.000	0.979	0.986	0.937	0.980	0.964	0.973
	Shape	1.000	0.999	1.000	1.000	0.999	1.000	1.000	0.999	1.000	0.999	1.000	0.999	1.000
	Phase	0.004	0.012	0.008	0.008	0.022	0.022	-0.002	0.028	0.034	0.034	-0.012	0.034	0.016
H3P-Near	Magnitude	0.957	0.996	0.982	0.985	0.982	0.966	0.950	0.967	0.953	0.858	0.974	0.784	0.946
	Shape	1.000	0.999	1.000	1.000	1.000	1.000	0.999	1.000	1.000	1.000	1.000	0.999	1.000
	Phase	-0.044	0.008	-0.012	0.036	0.012	-0.010	0.068	0.014	-0.016	-0.014	0.004	-0.010	0.003

Table A 2. H3 and H3P ATD lateral (Y), vertical (Z) excursions and apparent Neck (Head-T1), Thoracic Spine (T1-T8) and Lumbar Spine (T8-Pelvis) segments compression/tension

Number	ATD	Seating Position	Test	Head Y	T1Y	T8Y	Pelvis Y	Head Z	T1Z	T8Z	Pelvis Z	Neck	Thoracic Spine	Lumbar Spine
1849QR	H3	Trailing side	QR	1	1	1	1	36	45	49	42	-9	-4	7
1860QR	H3	Leading side	QR	99	74	61	43	41	49	53	45	-8	-4	8
1850	H3	Trailing side	LR	12	13	38	97	46	58	66	61	-11	-8	5
1861	H3	Leading side	LR	105	86	77	57	53	63	70	64	-10	-7	6
1848	H3	Trailing side	HR	102	85	91	106	60	70	78	70	-10	-9	8
1858	H3	Trailing side	HR	95	80	88	97	66	77	88	75	-11	-12	13
1863	H3	Leading side	HR	83	74	88	110	61	70	80	71	-9	-10	9
1862	H3	Leading side	HR	86	77	83	105	69	75	83	73	-6	-8	10
1860QR	H3P	Trailing side	QR	0	1	2	8	30	35	38	25	-5	-3	13
1849QR	H3P	Leading side	QR	129	101	79	51	30	41	44	31	-11	-3	13
1861	H3P	Trailing side	LR	14	17	41	104	36	48	54	39	-12	-6	15
1850	H3P	Leading side	LR	124	96	90	90	44	49	51	47	-5	-2	4
1862	H3P	Trailing side	HR	131	92	76	62	32	35	45	37	-3	-10	8
1863	H3P	Trailing side	HR	128	94	83	74	42	54	67	48	-12	-12	19
1858	H3P	Leading side	HR	109	87	104	129	55	61	68	53	-6	-7	15
1848	H3P	Leading side	HR	89	80	92	139	67	71	77	61	-4	-6	16

Table A 3. Difference between H3 and H3P ATD lateral (Y) and vertical (Z) excursions

Excursion difference(H3P-H3)									
Seating Position	Test	Head Y	T1Y	T8Y	Pelvis Y	Head Z	T1Z	T8Z	Pelvis Z
Trailing side	QR	0	0	1	7	*-6*	*-10*	*-11*	*-18*
Leading side	QR	30	27	18	8	*-11*	*-8*	*-9*	*-14*
Trailing side	LR	2	3	3	7	*-10*	*-10*	*-12*	*-22*
Leading side	LR	19	11	13	33	*-9*	*-14*	*-19*	*-16*
Trailing side	HR	30	7	-15	-44	*-28*	*-35*	*-33*	*-33*
Trailing side	HR	33	14	-4	-23	*-24*	*-22*	*-21*	*-28*
Leading side	HR	26	13	16	18	*-6*	*-9*	*-12*	*-18*
Leading side	HR	2	3	9	34	*-2*	*-4*	*-6*	*-12*

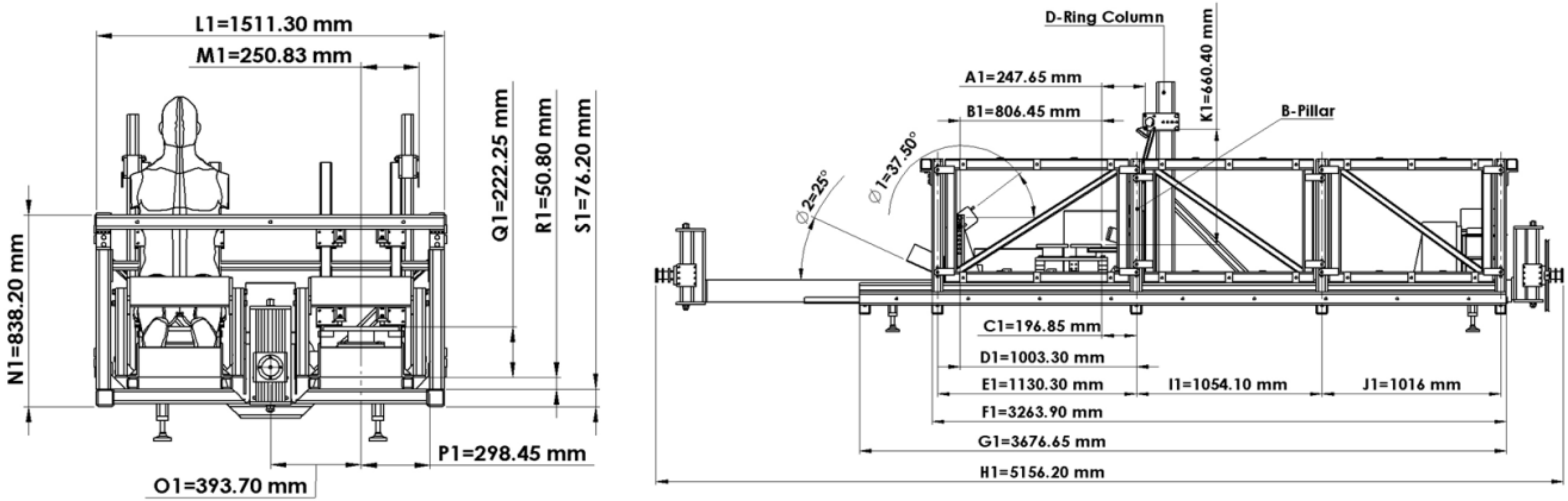

Figure A1. Parametric rollover buck: front view (left); side view (right)

A1

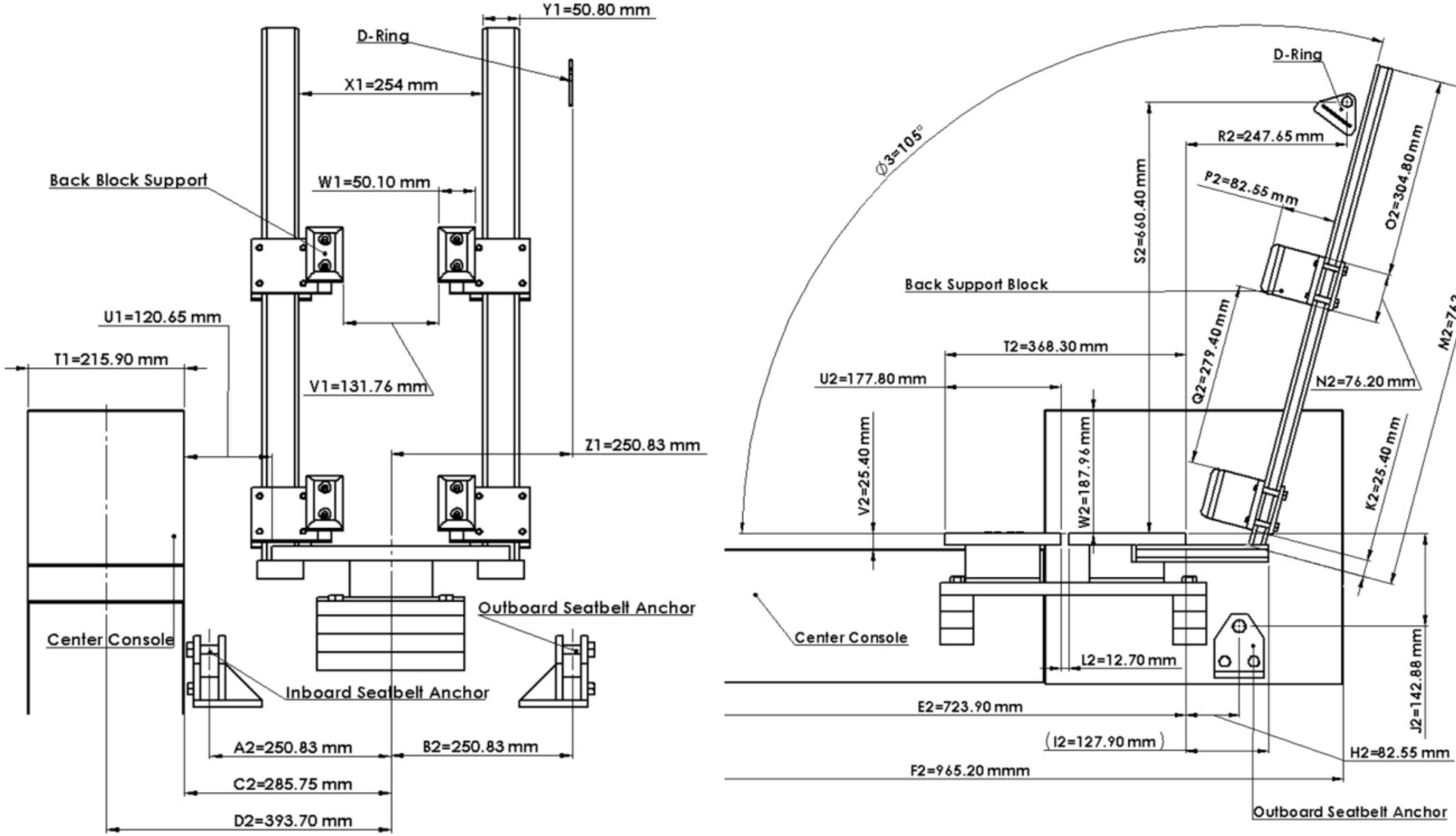

Figure A2. Rollover buck seat drawing: front view (Left); side view (Right)

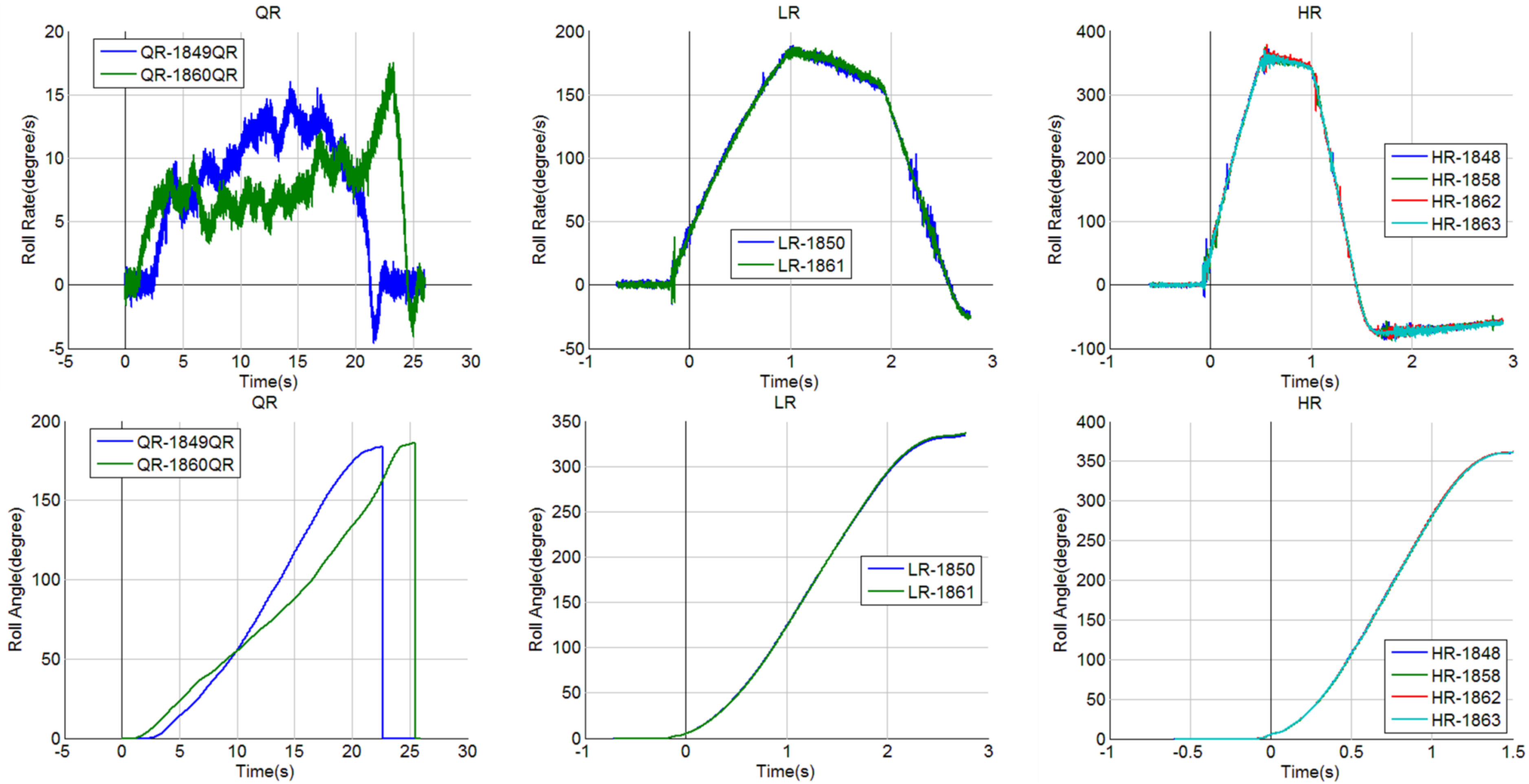

Figure A3 Rollover buck kinematics repeatability: Roll rate and roll angle time histories comparison for the QR, LR and HR tests.

ATD HEAD, T1, T8, PELVIS TIME HISTORY IN HR TESTS

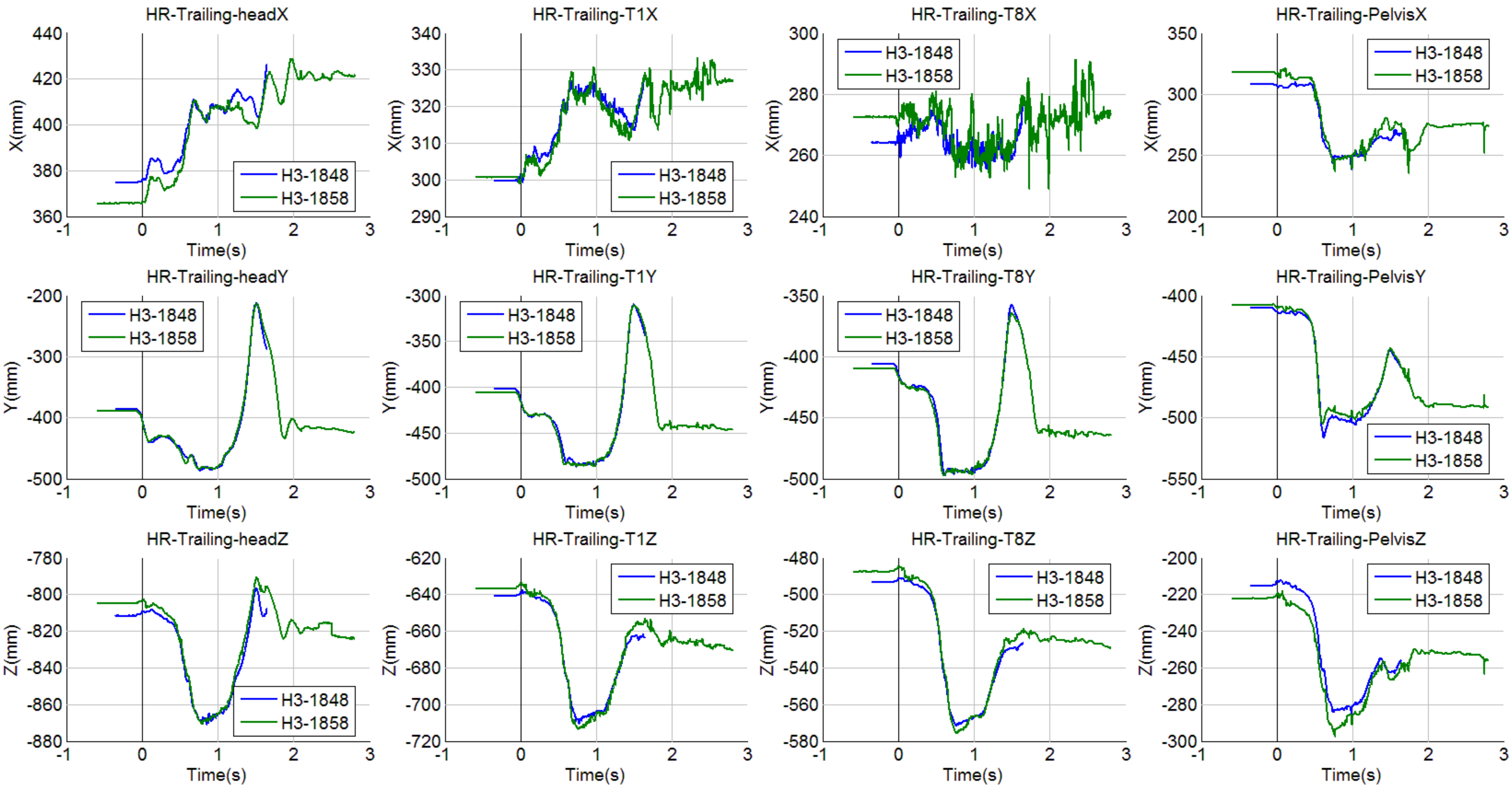

Figure A4. H3 ATD repeatability: ATD position time history in trailing-side seating position

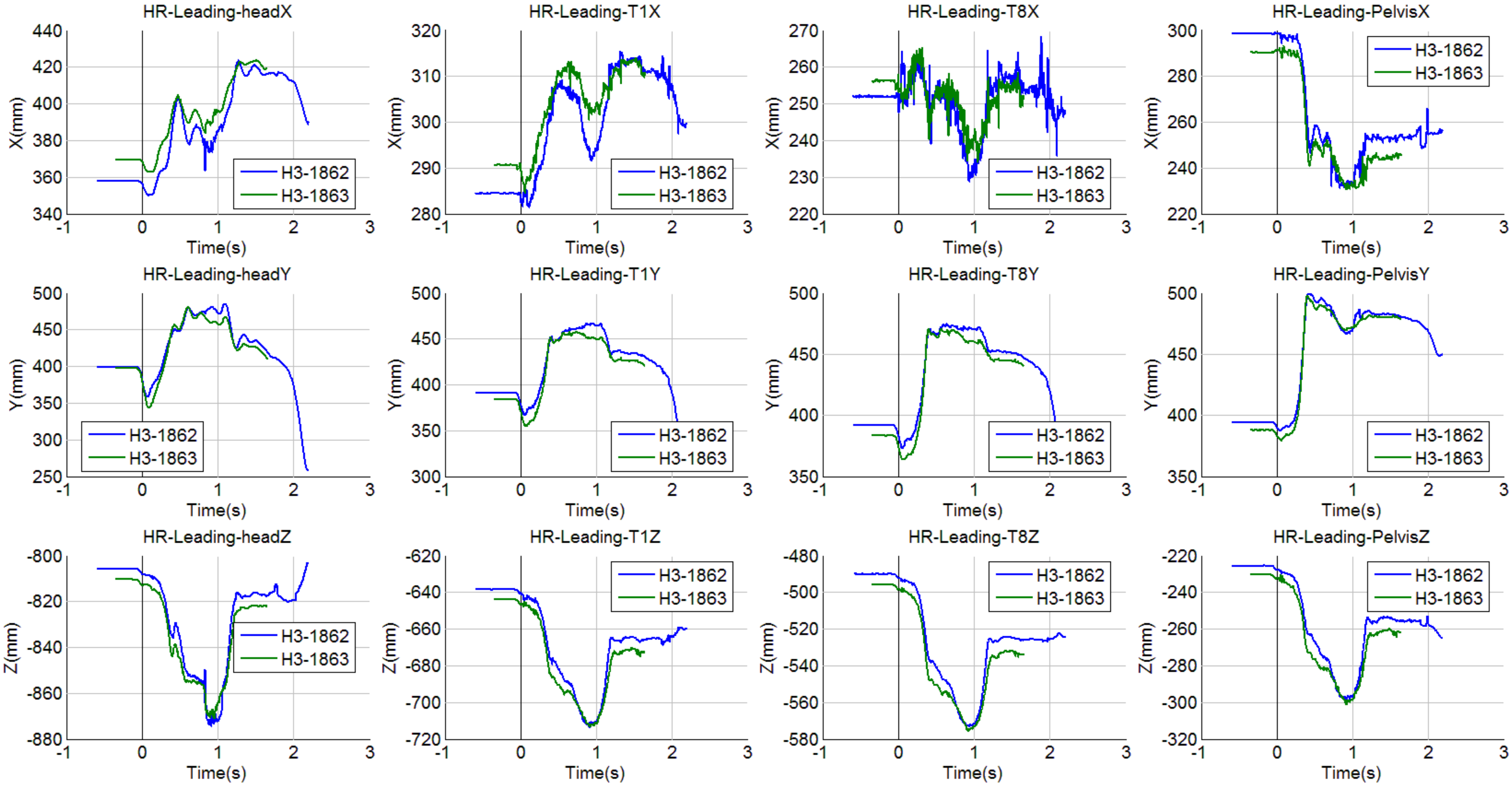

Figure A5. H3 ATD repeatability: ATD position time history in leading-side seating position

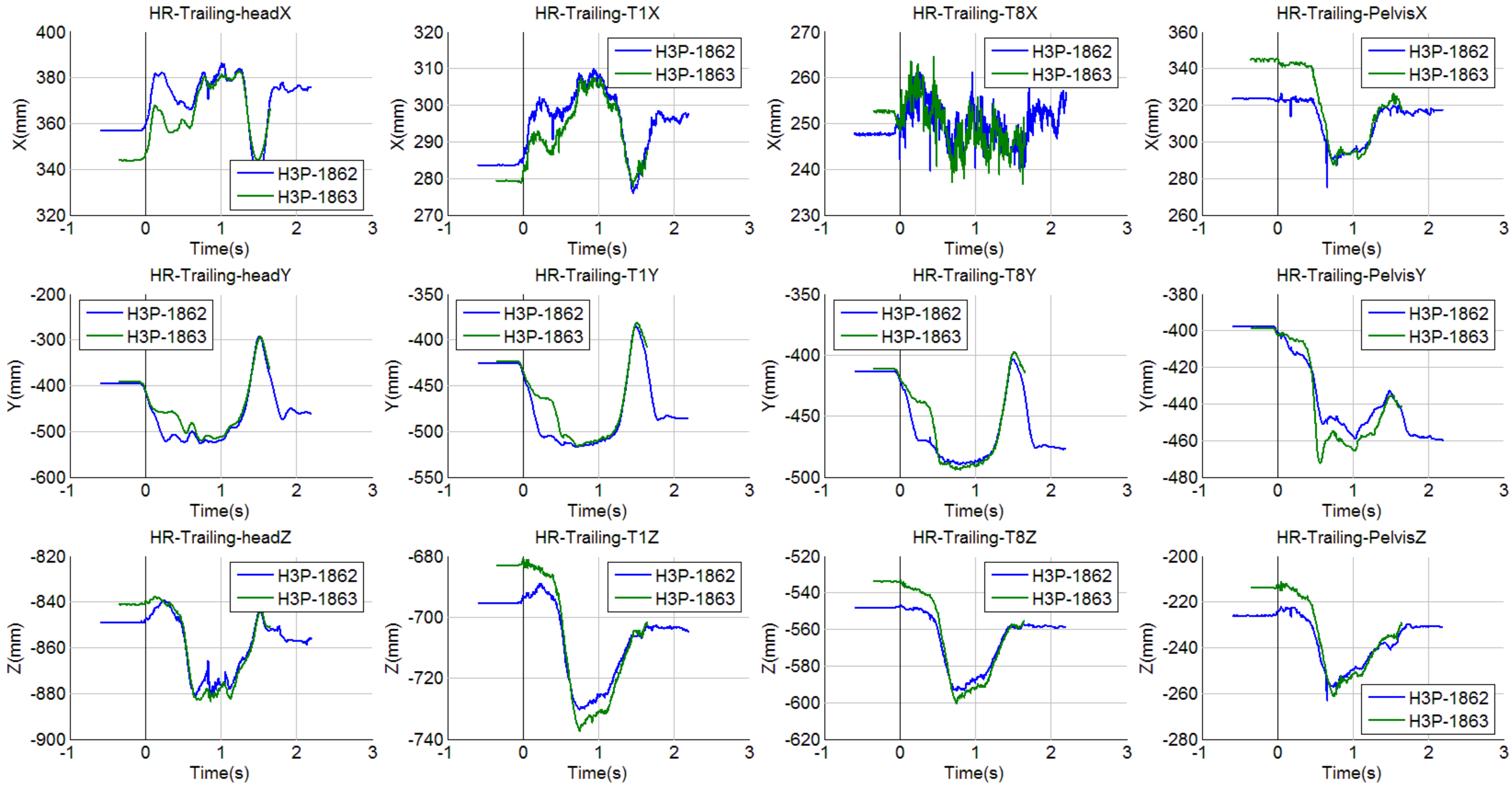

Figure A6. H3P ATD repeatability: ATD position time history in trailing-side seating position

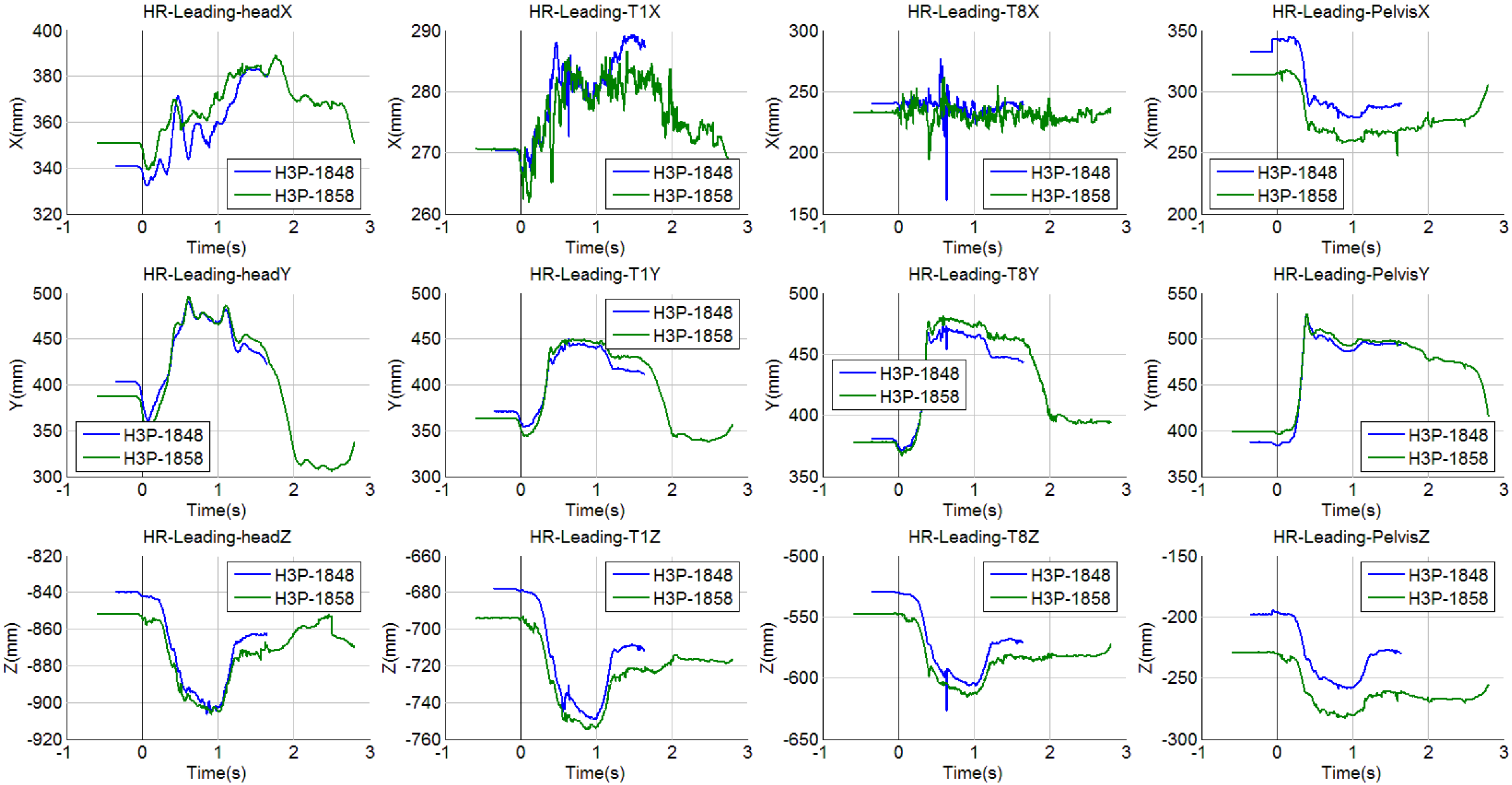

Figure A7. H3P ATD repeatability: ATD position time history in leading-side seating position

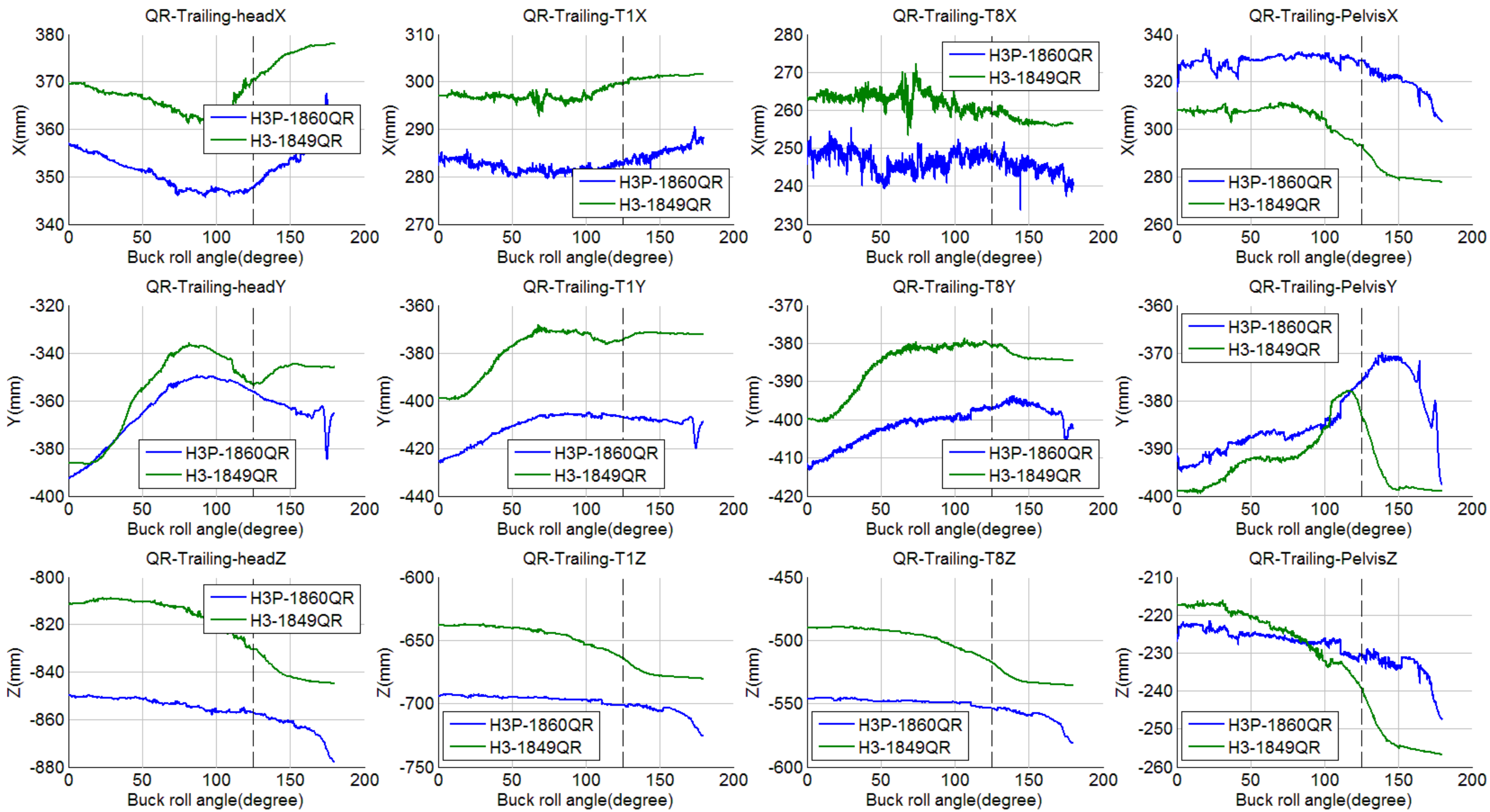

Figure A8. H3 and H3P ATD position VS buck rotational angle comparison in QR tests trailing-side seating position.

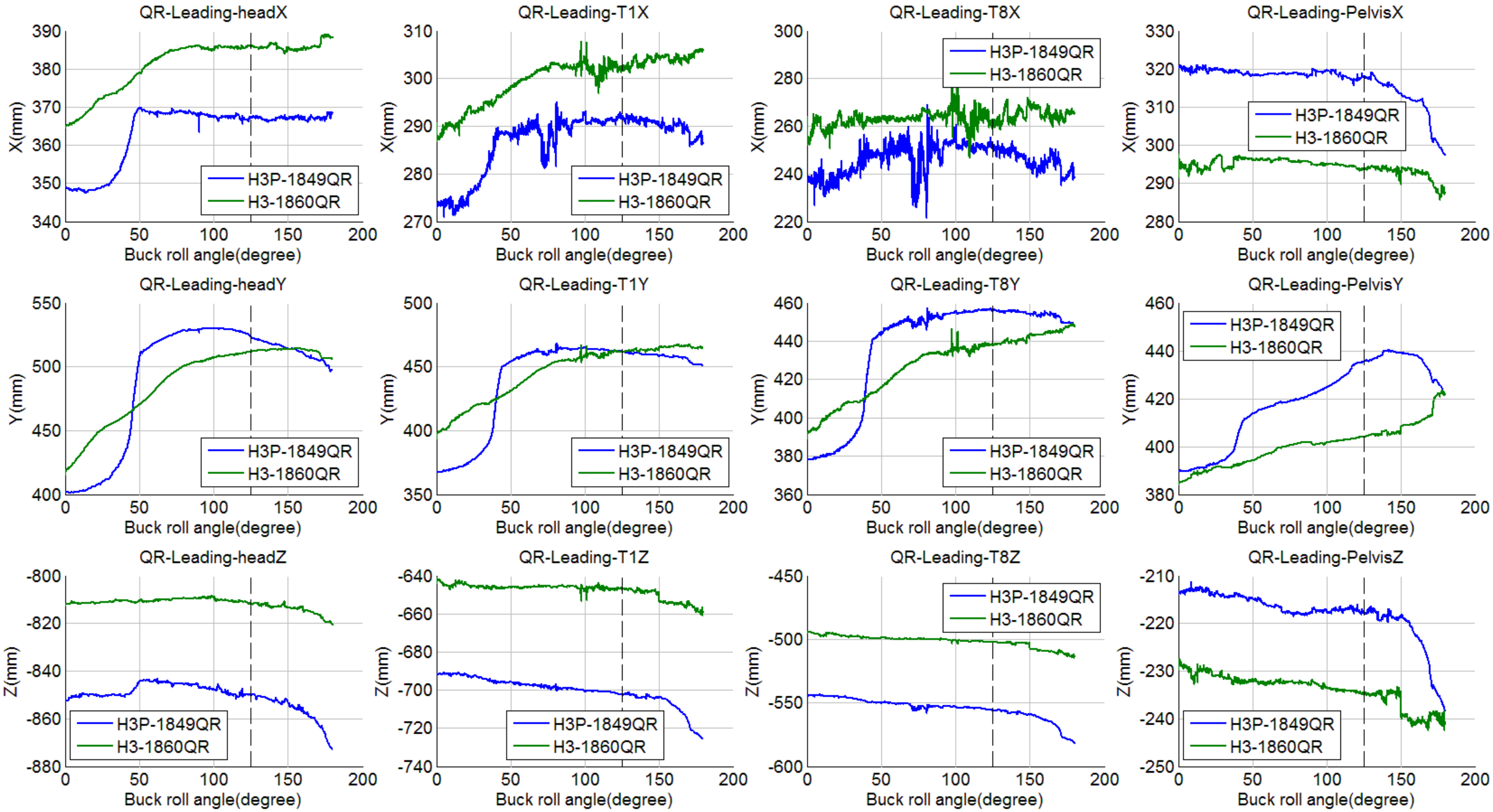

Figure A9. H3 and H3P ATD position VS buck rotational angle comparison in QR tests leading-side seating position.

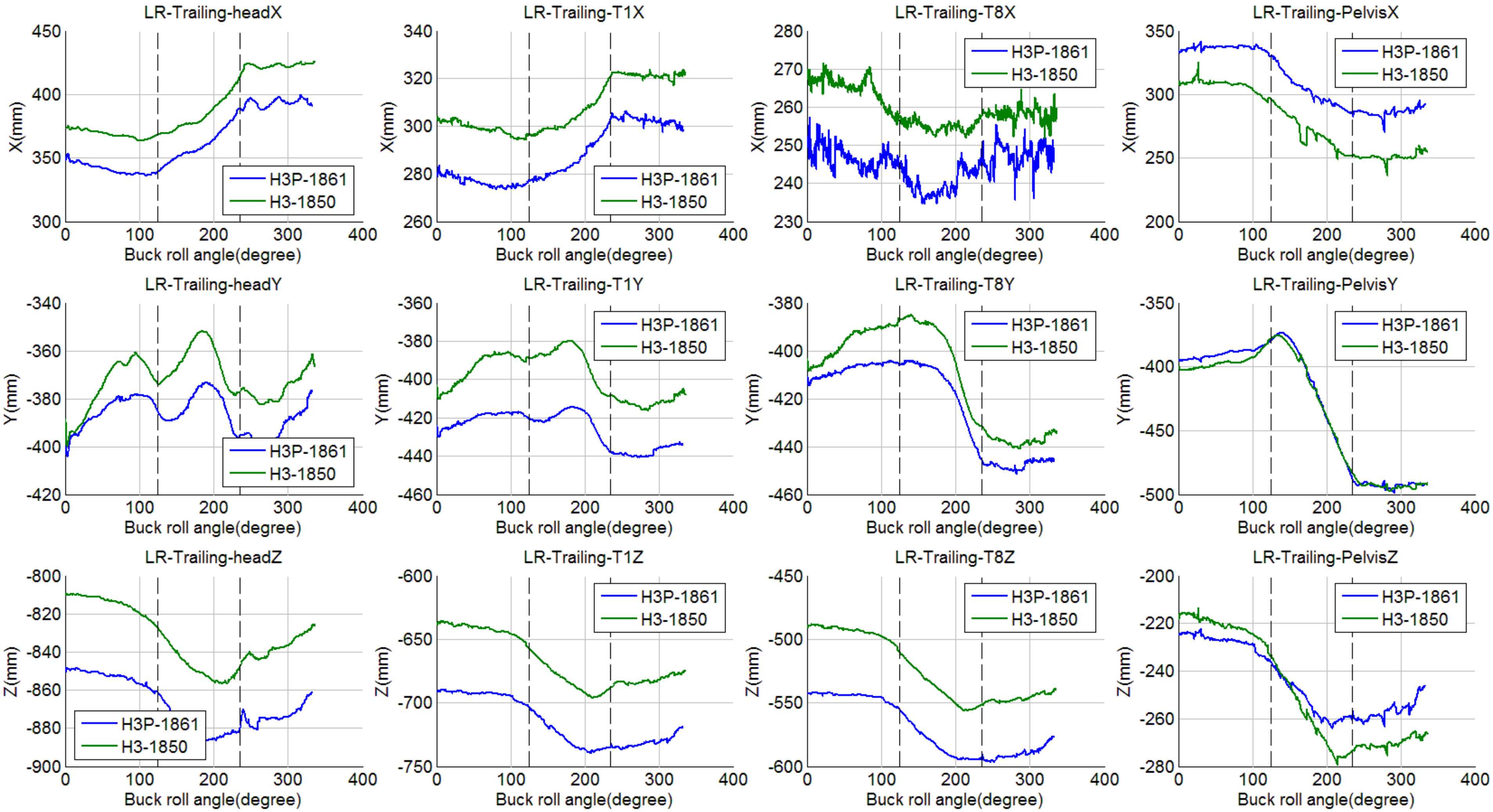

Figure A10. H3 and H3P ATD position VS buck rotational angle comparison in LR tests trailing-side seating position.

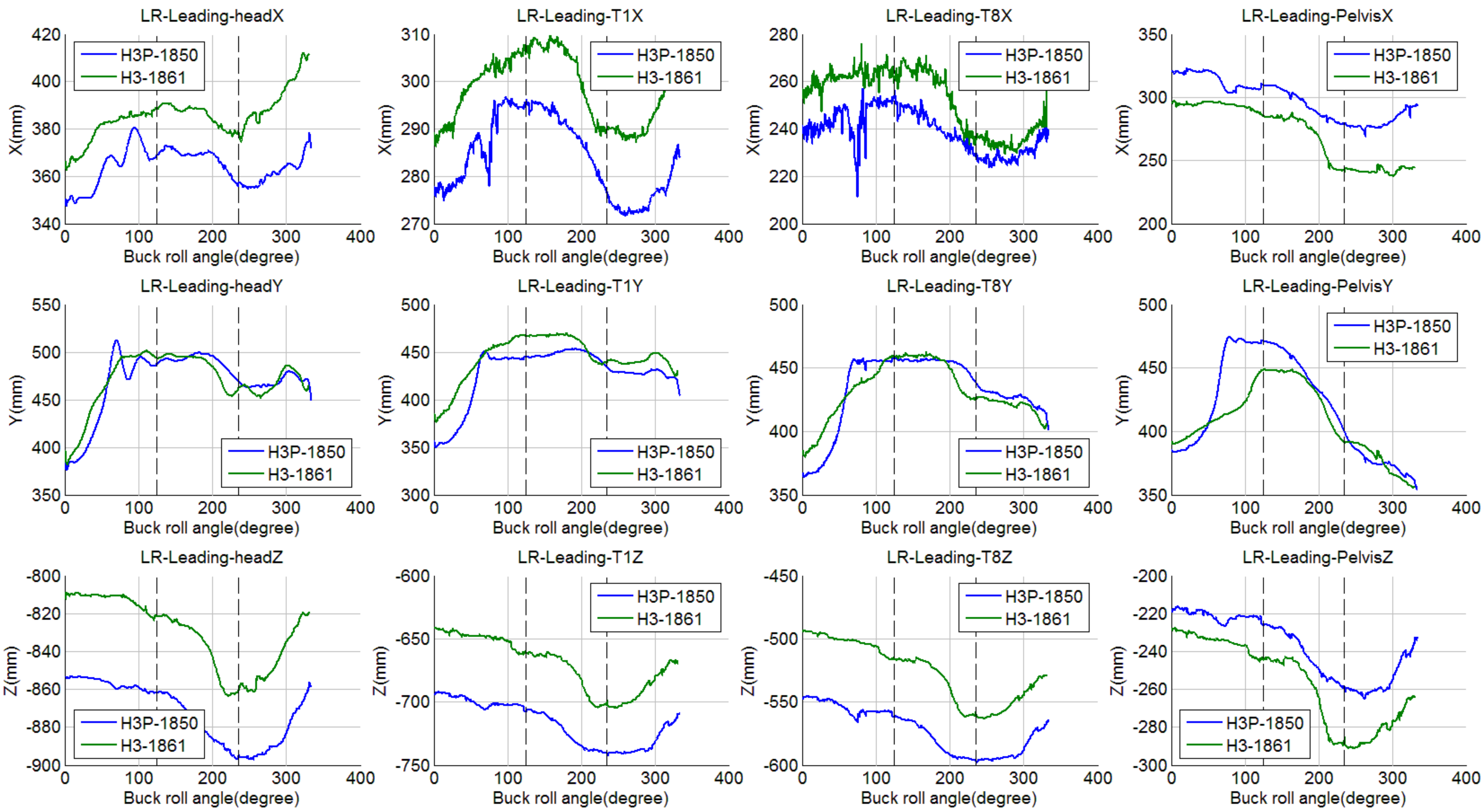

Figure A11. H3 and H3P ATD position VS buck rotational angle comparison in LR tests leading-side seating position.

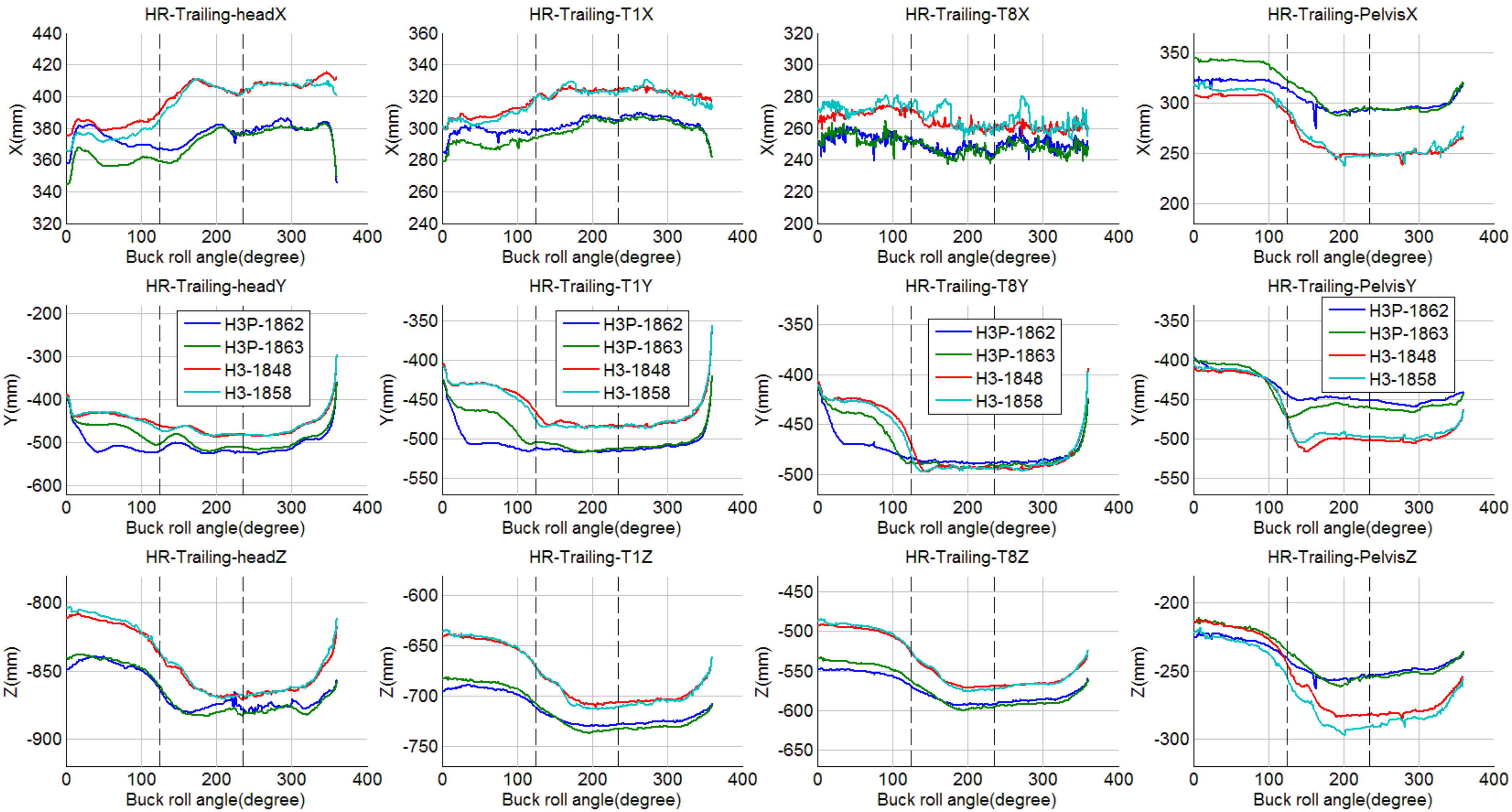

Figure A12. H3 and H3P ATD position VS buck rotational angle comparison in HR tests trailing-side seating position.

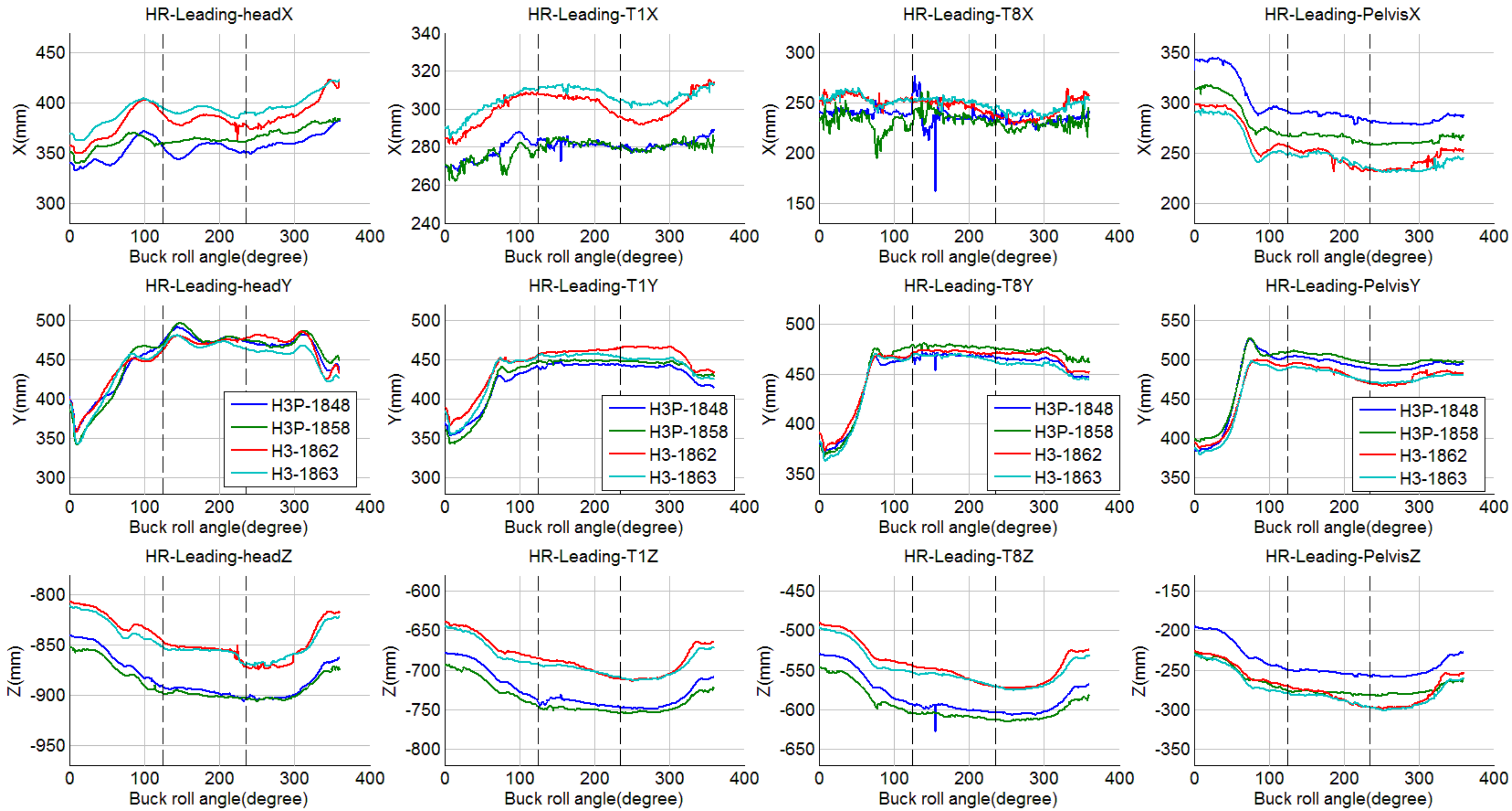

Figure A13. H3 and H3P ATD position VS buck rotational angle comparison in HR tests leading-side seating position.

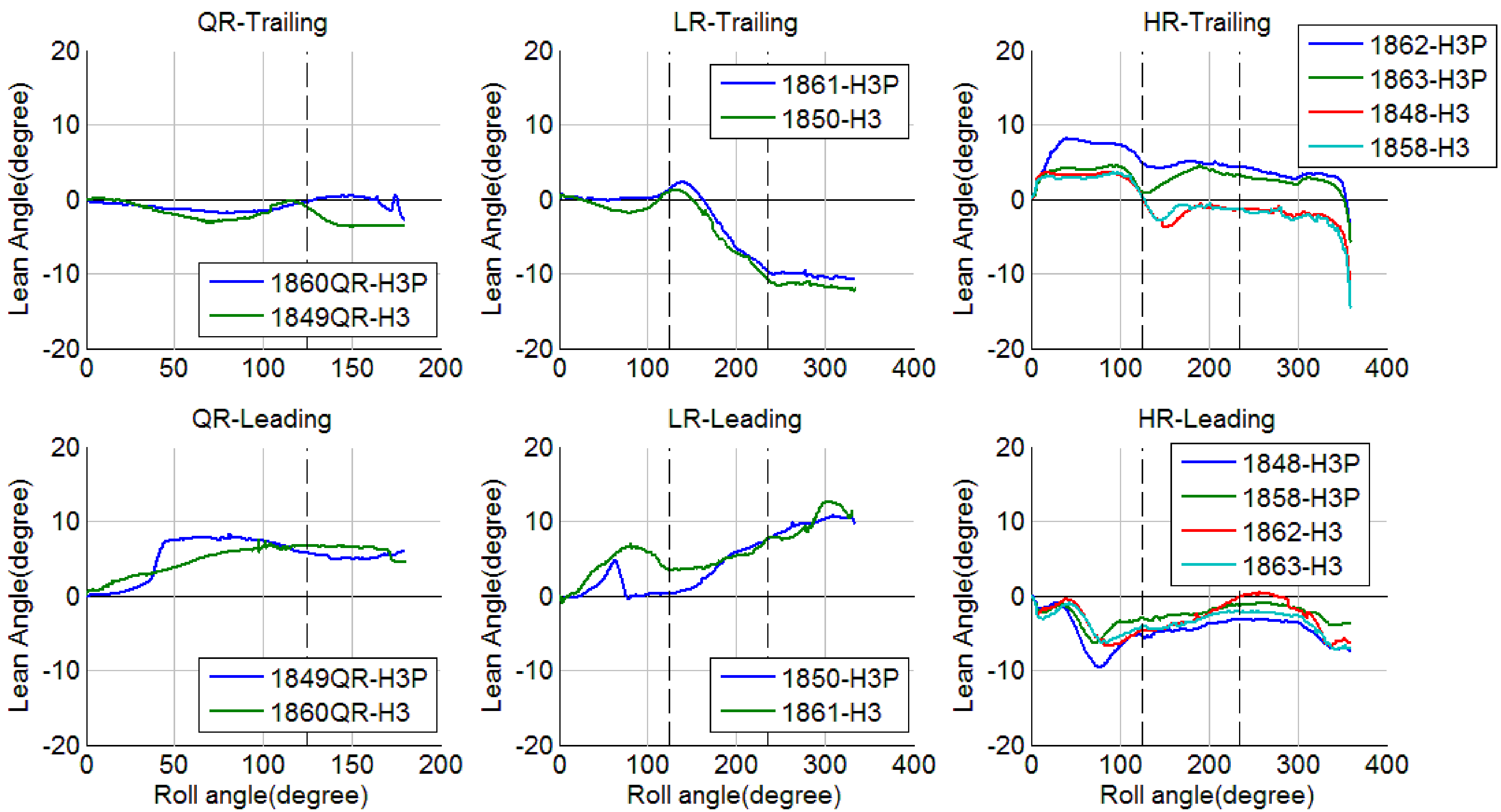

Figure A14. H3 and H3P ATD LeanAngle VS buck rotational angle (Positive value indicates outboard lean, negative value indicates inboard lean)

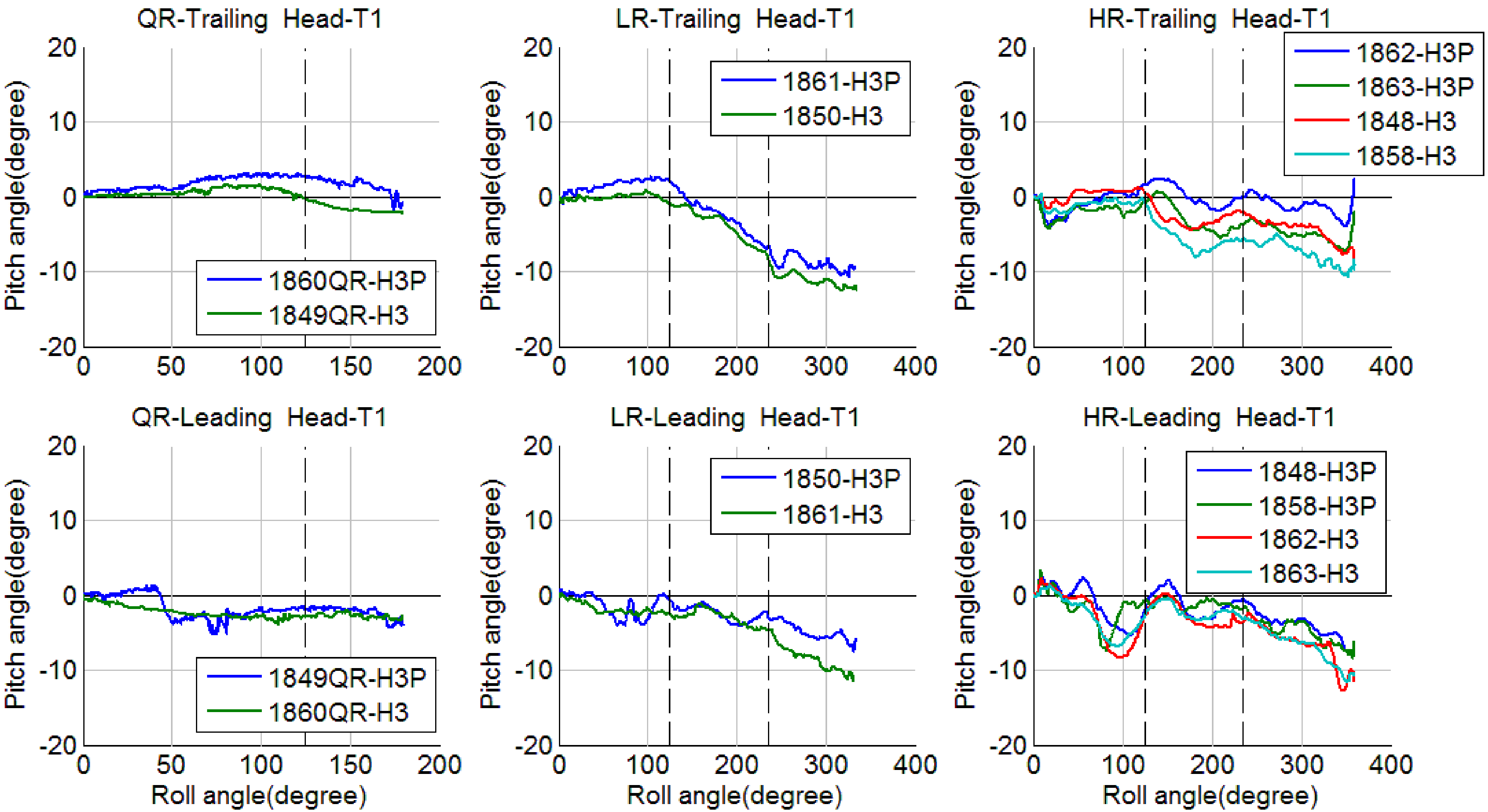

Figure A15. H3 and H3P ATD Head-T1 Pitch rotation VS buck rotational angle (Positive value indicates backward pitch rotation, negative value indicates forward pitch)

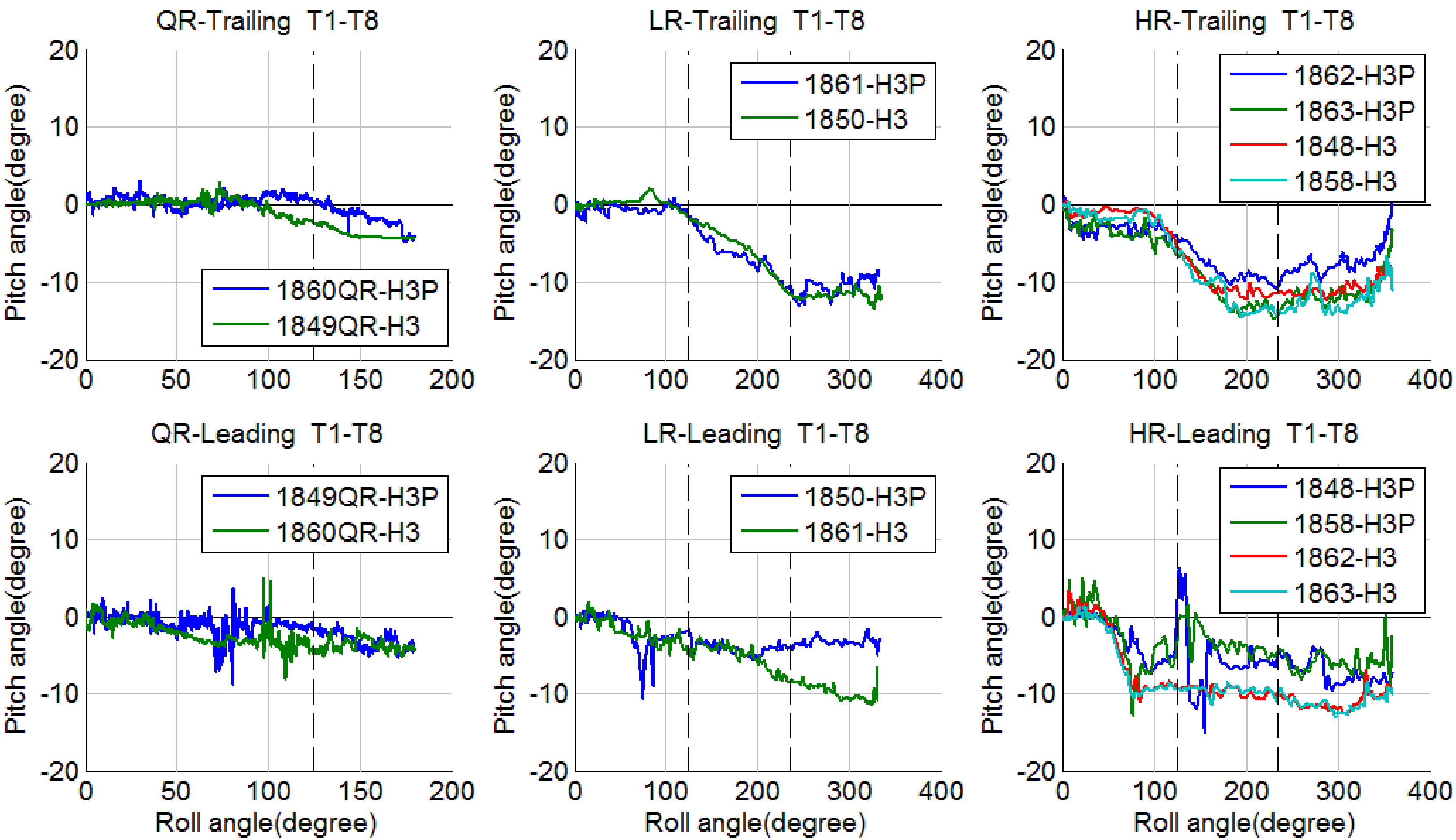

Figure A16. H3 and H3P ATD T1-T8 Pitch rotation VS buck rotational angle (Positive value indicates backward pitch rotation, negative value indicates forward pitch)

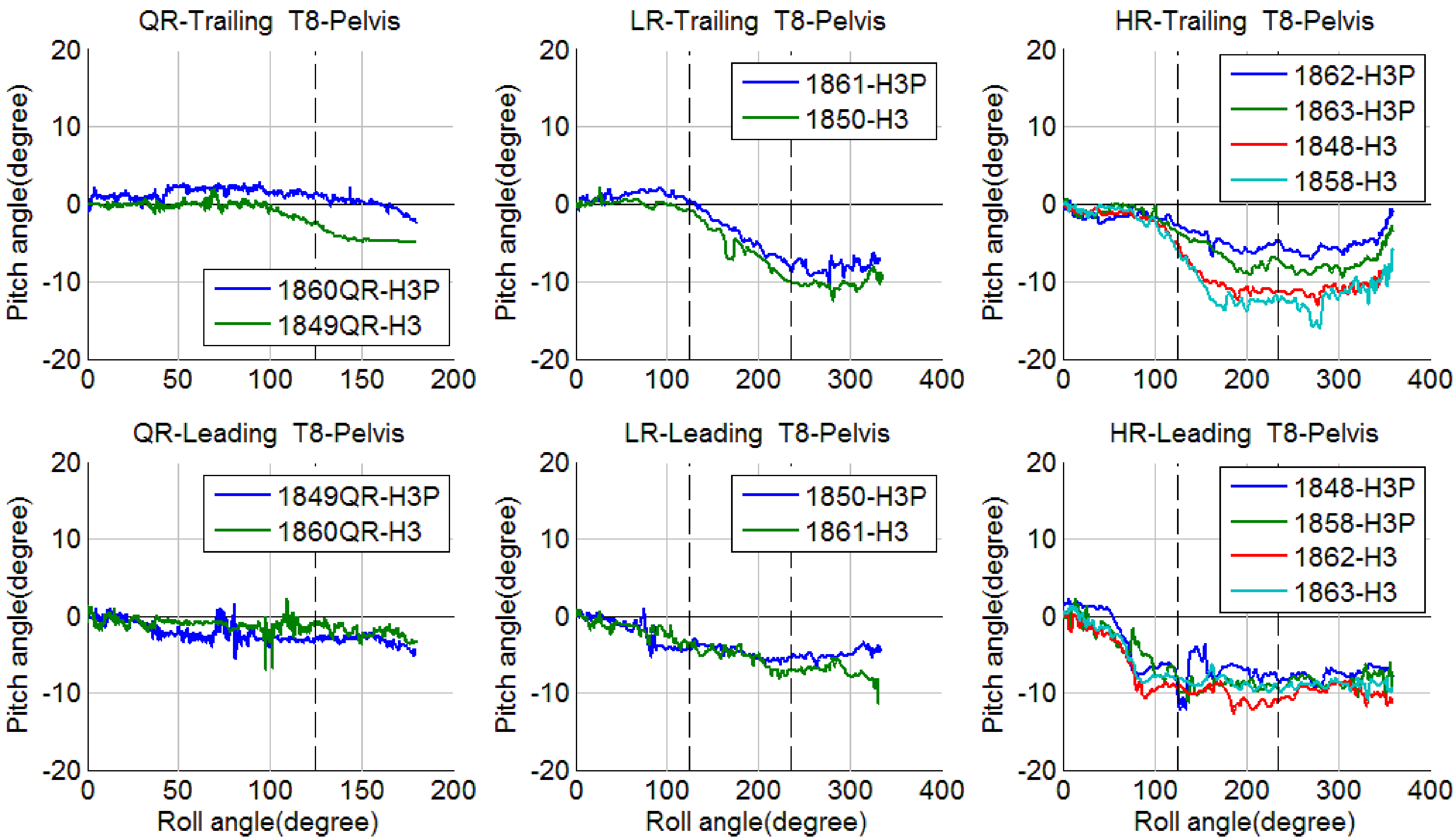

Figure A17. H3 and H3P ATD T8-Pelvis Pitch rotation VS buck rotational angle (Positive value indicates backward pitch rotation, negative value indicates forward pitch)

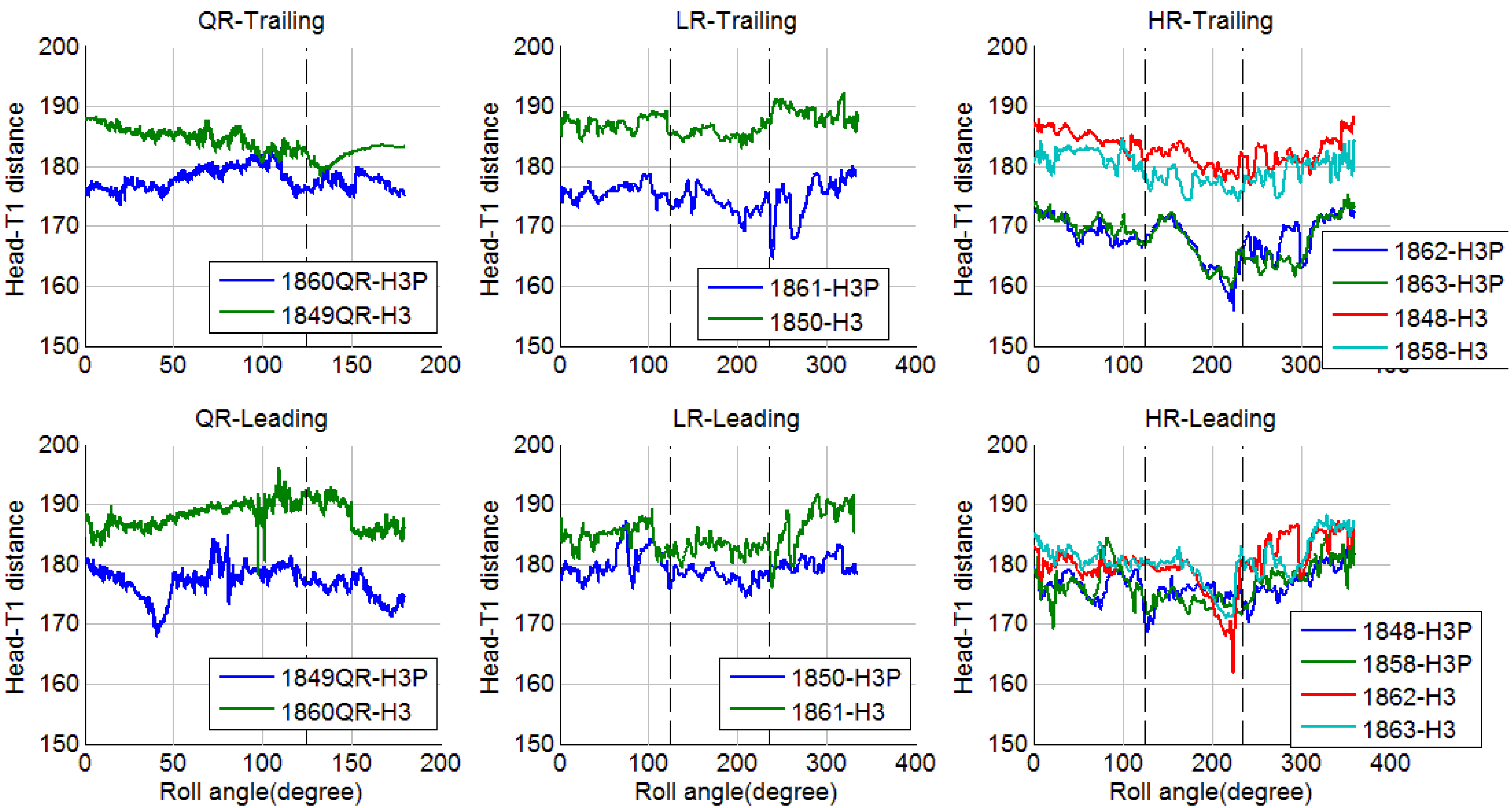

Figure A18. H3 and H3P ATD Head-T1 resultant distance VS buck rotational angle

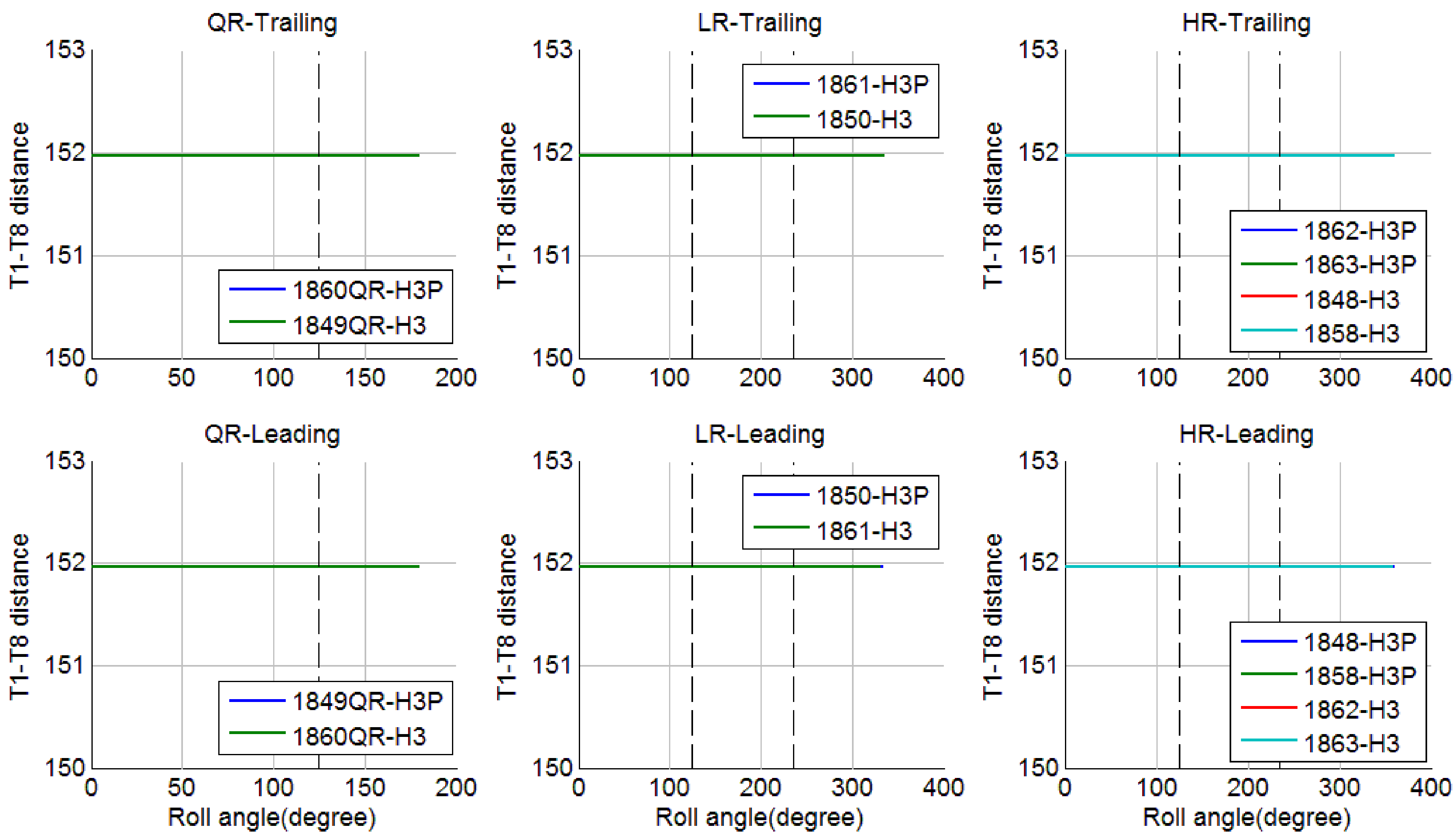

Figure A19. H3 and H3P ATD T1-T8 resultant distance VS buck rotational angle

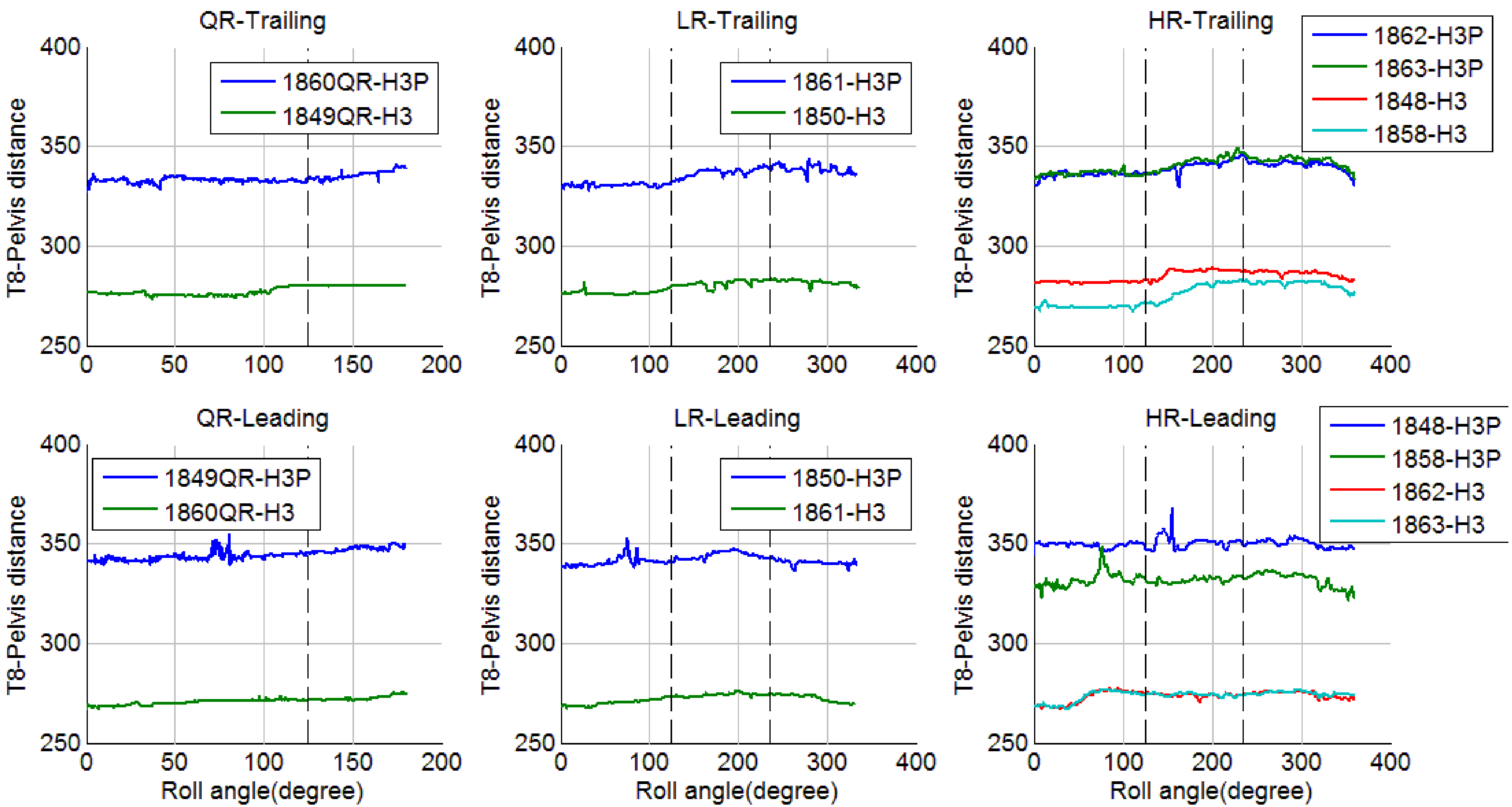

Figure A20. H3 and H3P ATD T8-Pelvis resultant distance VS buck rotational angle